Postprint of: Navrotsky A., Lee W., Mielewczyk-Gryn A., Ushakov S.V., Anderko A., Wu H., Riman R.E., Thermodynamics of solid phases containing rare earth oxides, The Journal of Chemical Thermodynamics, Vol. 88 (2015), pp. 126-141, DOI: 10.1016/j.jct.2015.04.008

Thermodynamics of Solid Phases Containing Rare Earth Oxides

Alexandra Navrotsky[a*], Wingyee Lee[a], Aleksandra Mielewczyk-Gryn[a,b], Sergey V. Ushakov[a], Andre Anderko[c], Haohan Wu[d], and Richard C. Riman[d]

This paper is dedicated to the memory of Lester R. Morss (1940 - 2014), a wonderful colleague and friend who contributed extensively to the thermodynamics, chemistry, and physics of lanthanides and actinides and to service to the Department of Energy.

[a]Peter A. Rock Thermochemistry Laboratory and NEAT ORU
University of California Davis
Davis CA 95616 U.S.A.

[b]present address: Department of Solid State Physics, Faculty of Applied Physics and Mathematics, Gdańsk University of Technology, Narutowicza 11/12, 80-233 Gdańsk, Poland

[c]. OLI Systems, Inc.
240 Cedar Knolls Road, Suite 301,
Cedar Knolls, NJ 07927-1621 U.S.A.

[d]. Department of Materials Science and Engineering,
Rutgers University
607 Taylor Rd
Piscataway, NJ 08854-8066 U.S.A.

* Corresponding Author: Alexandra Navrotsky, anavrotsky@ucdavis.edu, Tel: (530) 752-3292, Fax: (530) 752-9307

Highlights

- Rare earths (RE) are used in many applications involving multicomponent oxide materials with desirable optical, electronic, mechanical and chemical properties
- This paper summarizes thermodynamic properties of this diverse and extensive group of materials
- Ionic size is a major factor in determining the systematics of RE phase stability

Keywords: Multicomponent rare earth oxides, review, rare earth oxide thermodynamics

Abstract

Rare earth elements (RE) are incorporated into a large variety of complex oxide phases to provide tailored mechanical, electrical, optical, and magnetic properties. Thermodynamics

control phase stability, materials compatibility in use, corrosion, and transformation. This review presents, in one compilation, the thermodynamic properties of a large number of such materials and discusses systematic trends in energetics and the factors controlling stability.

1. Introduction

The rare earth (RE) elements (often defined as the lanthanides plus yttrium) are technologically important in applications ranging from phosphors to fuel cells, magnets to medicine, superconductors to cell phones, turbines to thermoelectrics. They are considered "rare", not because of very low geochemical abundance, but because there are few natural occurrences where RE are present in high concentrations. Their mining, beneficiation, separation, and processing involve many steps and can have a negative environmental impact, which is one of the factors driving such industry overseas, especially to China, where rare earth ores are abundant and environmental regulation has been much more lenient than in the U.S.A. Technological uses of RE range from applications requiring major RE constituents in magnets to trace amounts in light emitting diodes (LED), with specific processing tailored to particular elements and devices. Rare earths are also major fission products in the nuclear fuel cycle. Finally, recovering rare earths after use can be difficult, labor intensive, and a source of pollution. Thus the "cradle to grave" rare earth cycle is fraught with challenges. Rare earths are considered "strategic" or "critical" because their supply is limited and often geopolitically controlled yet a shortage would impact many industries and potentially disrupt our technology-dependent society. Indeed rare earths are a major focus of the recently established U.S.

Department of Energy Hub, the Critical Materials Institute dedicated to the more efficient use of critical materials.

The processing of rare earths and their incorporation into devices are governed by what is thermodynamically possible, and sustainable technology needs thermodynamically and kinetically efficient pathways using minimum energy and causing the least environmental harm. Thus the thermodynamic properties of rare earth oxide materials must be known and used to develop industrial best practices.

Rare earths, as all elements, come from the Earth. Specific RE minerals are usually minor constituents of rocks and RE are often incorporated in such minerals in minor concentrations, with several RE occurring together. The major commercially exploited ore is bastnasite, a complex RE carbonate hydroxide fluoride, followed by monazite and xenotime (phosphates), and several others (see table 1). In addition, rare earth materials are significant byproducts, currently not reclaimed, in the waste produced in other mineral processing technologies. For example, the production of fertilizer (ammonium phosphate) from "phosphate rock" (mainly apatite with significant RE content (as well as radioactive elements U, Th, and Ra) results in thousands of tons of a "phosphogypsum" waste, a calcium sulfate incorporating RE and phosphate impurities. For more efficient and environmentally sustainable mining and ore processing, as well as reclaiming RE from current waste streams, complete thermodynamic data are needed.

The purpose of this paper is to provide, in a single source, an overview of thermodynamic properties of crystalline rare earth oxide systems, with emphasis on families of multicomponent compounds with specific structures (*e.g.* perovskite, fluorite, garnet, apatite) often having distinct technological applications (*e.g.* piezoelectrics, superconductors,

multiferroics, optical materials). The structures and properties of different families of rare earth materials are discussed briefly and general trends in thermodynamic properties, useful for interpolation, extrapolation, and prediction, are identified. The literature on thermodynamic properties of different families of ternary and higher RE oxide materials is scattered in primary scientific journals and this is the first major effort, to the authors' knowledge, to bring it together. This review focuses on experimentally determined thermodynamic properties, although computational methods, especially density functional theory approaches, are becoming more important and successful in evaluating thermodynamic properties of complex solids containing rare earth oxides. The Navrotsky group in the Peter A. Rock Thermochemistry Laboratory at UC Davis has done extensive work over the last two decades in determining enthalpies of formation in multicomponent rare earth oxide systems and these studies provide much of the data summarized in this paper.

2. Binary Oxides

A detailed review of structures and properties is given by [1]. Thermodynamic properties have been reviewed comprehensively by Morss and Konings [2]. The most common RE oxidation state is +3, giving the formula RE_2O_3 (or, per one metal, $REO_{1.5}$).Thermodynamic properties of the trivalent binary oxides are summarized in table 2. The trivalent oxides are refractory, high melting, and polymorphic. At room temperature, trivalent rare earth oxides are found in hexagonal (P32/m), monoclinic (C2/m) and cubic (la3) structures, denoted as A, B and C. In the C-type structure, rare earths (Lu to Gd and Y) are octahedrally coordinated by oxygen, and the structure can be viewed as a vacancy ordered variant of fluorite. Both six and seven

coordination are present in the B-type, typical for the middle of rare earth series. The coordination number for La to Nd in the A-type structure is seven. Above 2000 °C all sesquioxides, save Lu_2O_3, transform to another hexagonal phase. (P63/mmc, H-type), which is closely related to the A-type. Before melting, La to Dy oxides undergo yet another phase transformation into a cubic (Im3m, X-type) phase. The H and X phases are not quenchable to room temperature. Experimental thermodynamic information for high temperature phase transitions and fusion of RE_2O_3 phases is scarce but available values for phase transition thermodynamics are summarized in table 3.

Cerium forms two major oxides, CeO_2 and Ce_2O_3 and can be incorporated into multicomponent oxides in both the trivalent and tetravalent states, *e.g.* Ce^{3+} in $CePO_4$ and Ce^{4+} in $BaCeO_3$ perovskite. Praseodymium and terbium form several complex phases between RE_2O_3 and REO_2 in composition. Rather than being non-stoichiometric and disordered, these represent a series of ordered materials, with ordering based on accumulation of oxygen vacancies in specific crystallographic planes whose spacing determines the structure and stoichiometry [3]. Closely spaced in enthalpy and free energy [4; 5], they define a complex and dense landscape of accessible structures. Tetravalent praseodymium is also present in a variety of $APrO_3$ (A = alkaline earth) perovskites [6]. In addition to Eu_2O_3, europium forms a divalent oxide with rock salt structure, EuO, which undergoes an electronic phase transition at high pressure with a volume decrease of about 10 % with no change in the basic rock salt structure [7].

Thermodynamic data for the formation of binary RE oxides are summarized in table 3. When multiple values are reported, the ones we consider most reliable (generally from the Morss and Konings (2004)[2] review) are given in bold.

3. Perovskites and Related Structures

The perovskite structure of stoichiometry ABO_3, shown in figure1a, consists of a framework of corner sharing octahedra (containing the smaller "B" cations), with the cavities between them defining a large central site that contains the larger "A" cations. If the perovskite is cubic and undistorted, the A-site has 12-fold coordination. A geometric factor, the Goldschmidt tolerance factor, t, describes the misfit of A-O and B-O bond lengths for the ideal cubic perovskite structure. If "t" deviates significantly from unity, distortions occur, largely involving tilting of octahedra (see figure1b); the coordination number of the A-site cation decreases to 8, decreasing the symmetry from cubic to tetragonal, orthorhombic, or even lower. There is a large family of rare earth perovskites of the 3-3 charge type (both A-site and B-site cations trivalent). They can be represented as $REMO_3$, with M^{3+} = Al, Ga, Sc, In, Cr, Mn, Fe, Co. They have been investigated intensively because of their useful electrical and magnetic properties [8; 9]. Double rare earth perovskites, with a larger RE on the A-site and a smaller one on the B-site are of marginal thermodynamic stability but their energetics fit the trend of enthalpy vs. tolerance factor defined by more stable perovskites [10].

The tolerance factor, accounting for bond length or size mismatch, is the major factor controlling the enthalpy of formation of 3-3 perovskites from their binary oxides (see figure 2a). As "t" deviates from unity, the perovskites become more distorted and less stable [11; 12; 13; 14; 15].

The distortions from cubic symmetry driven by size mismatch depend on composition and temperature, with first order or higher order transitions among them. In general the enthalpies associated with such transformations is small (< 5 $kJ \cdot mol^{-1}$) [16; 17] but the symmetry

changes can result in major changes in physical, magnetic, and optical properties and microstructure.

Substitution of large divalent ions (Sr,Ba) for RE on the A-site and of Mg^{2+} for M^{3+} on the B-site leads to defect perovskites. Two modes of charge balance are possible: creation of oxygen vacancies:

$$RE^{3+}_A \rightarrow A^{2+}_A + 0.5\ (vacancy)_O \qquad (1)$$

$$M^{3+}_B \rightarrow M'^{2+}_B + 0.5\ (vacancy)_O \qquad (2)$$

and, when the trivalent transition metal, especially manganese, can be oxidized easily to the tetravalent state, oxidation or creation of electron holes:

$$RE^{3+}_A + M'^{3+}_B \rightarrow A^{2+}_A + M'^{4+}_B \qquad (3)$$

The balance between these mechanisms depends on the nature of M, temperature, and oxygen fugacity. The resulting perovskites can be ionic, electronic, or mixed conductors and have been studied extensively for these properties. Studies of thermodynamic properties of such solid solutions are summarized in table 4.

Perovskites of the 2-4 charge type, $A^{2+}B^{4+}O_3$ (A = Ca, Sr, Ba, Pb and B = Ti, Zr, Hf, Ce and Pr) are also well known. Their thermodynamics of formation from the binary oxides also appears governed largely by the tolerance factor (Fig 2b) [12; 18]. The praseodymium

perovskites are significantly more stable than predicted from the energetics of perovskites containing other tetravalent ions, and this added stability is attributed to electronic factors [6].

In minerals the substitution of RE into perovskites is often charge balanced by the incorporation of niobium or tantalum. Some of these substitutions and the mineral names associated with them are listed in table 5. The thermodynamic factors governing these substitutions are not well known and are an area of current research. Such data are needed for RE to be efficiently extracted from these refractory minerals.

The perovskite structure is a starting point for the creation of more complex structures by intercalating non-perovskite layers between perovskite-like ones. This generally changes the stoichiometry: an important example is the K_2NiF_4 or RE_2MO_4 (M^{2+} = Fe, Co, Ni, Cu) type, in which perovskite and rock salt layers alternate. These structures can be doped with divalent ions (Sr or Ba) substituting for RE), and charge balance is maintained by a competition between creating oxygen vacancies and oxidizing M^{2+} to M^{3+}, although the electron hole so created may be delocalized to involve oxygen p-states as well As in other perovskites discussed above, the relative importance of these two mechanisms depends of the nature of M, temperature, and oxygen fugacity. Indeed Ba-doped La_2CuO_4 was the first high T_c oxide superconductor discovered, and such systems have critical temperatures near 40 K. Thermodynamic studies of this family of solid solution systems are summarized in table 4.

Superconductors with T_c near 90 K are found in the yttrium barium copper oxygen system (YBCO) and related materials can be made containing different RE [19; 20]. Thermochemical studies of the "123" compound $YBa_2Cu_3O_x$ ($6 \leq x \leq 7$) show that the enthalpy of oxidation is constant across the whole range ([21; 22], despite that the formal oxidation state of copper changes from an average value of 1.67 (one Cu^+ and two Cu^{2+}) at x = 6 to 2.00 (all

Cu^{2+}) at x = 6.5 to 2.33 (formally one Cu^{3+} and two Cu^{2+}) at x = 7. It is also noteworthy that the enthalpy of oxidation in YBCO and Ba-doped La_2CuO_4 is similar and close to the enthalpy of oxidation of BaO to BaO_2 [23].Whether this thermodynamic similarity has implications for the nature of hole states in these materials is unclear. In the $REBa_2Cu_3O_7$ series, the enthalpy of formation from binary oxides is linearly related to ionic size (figure3), with no anomaly at praseodymium, suggesting that a change in the oxidation state of Pr is not the reason that compound fails to show superconductivity while all others in the series do so [24]. These data provide thermochemical constraints on the phase diagrams, chemical behavior and possible charge distributions in the normal state.

4. Fluorite and Pyrochlore

The fluorite structure of stoichiometry AO_2 is adopted by CeO_2, UO_2, and ThO_2 at ambient temperature and by ZrO_2 and HfO_2 at high temperature. It consists of an array of cubes with oxygen at the corners and the cation in the center of half the cubes (Figure4). This structure is the parent (aristotype) of several families of more complex structures, in which ionic substitutions, distortions, and order-disorder define structure and properties. A major characteristic of the fluorite structure is the relative ease, from an energetic point of view, of forming structures with oxygen vacancies. The high temperature fluorite structures of ZrO_2 and HfO_2 can be "stabilized" to room temperature by the substitution of trivalent RE, with one oxygen vacancy formed for every two cations substituted. The materials are oxide ion conductors, the most familiar example being yttria stabilized zirconia (YSZ), in commercial use in applications such as oxygen sensors for car exhausts and steelmaking, gas separation membranes, solid oxide fuel cell (SOFC) electrolytes, and thermal barrier coatings for aircraft

engines. Though the concentration of vacancies is determined by the extent of RE doping, they associate into clusters as their concentration increases, and the ionic conductivity often shows a maximum at a given composition. The thermodynamics of formation of such AO_2-$REO_{1.5}$ solid solutions is complex [25; 26; 27; 28]. Positive enthalpy contributions from size mismatch (lattice strain) and negative contributions from cluster formation are competing factors. The entropy of mixing is very difficult to calculate because there is short range order on both cation and anion sub-lattices, and clusters involve cations, anions, and vacancies. Furthermore these factors all depend on temperature as the clusters undergo some disordering with increasing temperature. These points are discussed in detail in the papers listed in table 4.

In addition to the partially disordered defect structures discussed above. A number of fully ordered structures can be derived from fluorite. The C-type rare earth oxide structure is a ordered fluorite variant, with oxygen vacancies fully ordered in the 111 direction. Its $REO_{1.5}$ stoichiometry means that 25 % of the anion sites are vacant, but because the vacancies are ordered, they are considered part of the structure and not defects, and there is no configurational entropy. Whether some C-type rare earth oxides disorder to the fluorite structure at high temperature before they melt is still controversial.

The pyrochlore structure (figure 5) [29] of $RE_2B_2O_7$ (B =Ti, Zr, Hf, Sn) stoichiometry is an ordered variant, with two distinct cationic (*16c/16d*) and anionic (*8b/48f*) sub-lattices, of the disordered defect fluorite structure. The positional "*x*" coordinate of the *48f* 'O' site is unconstrained and it can be considered a measure of how "fluorite-like" or "pyrochlore-like" a particular material is, since the transformation between defect fluorite and pyrochlore appears to occur gradually, influenced by temperature and also by radiation damage [30]. Table 3

summarizes enthalpies of formation of RE pyrochlores and table 6 gives references to the energetics of order-disorder.

Natural pyrochlore minerals are complex in composition and stoichiometry. Some of their charge balanced substitutions are given in table 5. As in perovskites, substitution for Ti of a trivalent RE and a pentavalent ion like Nb and Ta is a major mechanism for RE incorporation, but the thermodynamics of such substitutions are poorly known.

Rare Earth elements are major fission products in nuclear reactors, and UO_2 is the main nuclear fuel. Furthermore fuel cladding is a zirconium alloy (zircalloy). Thus understanding substitution of RE in defect fluorite and pyrochlore structures in UO_2-ZrO_2-Re_2O_3 systems is important to nuclear energy production as well as to nuclear waste disposal. Furthermore Ce^{4+} is considered a useful chemical analogue to Pu^{4+} because of similar ionic radii, and CeO_2 is used extensively in surrogate studies of mixed oxide (PuO_2-UO_2) fuels and issues related to plutonium disposition**.** Thus there is intersection and synergy between work on solid oxide fuel cells and nuclear energy, with doped CeO_2 playing a central role in both fields.

5. Garnet

The garnet structure, well known from mineralogy, with the general formula $A_3M_2T_3O_{12}$, contains divalent ions (transition metals and calcium) on distorted cubic (A) sites, smaller trivalent ions (Al, Fe, Cr) on octahedral (M) sites and small tetravalent ions (Si) on tetrahedral (T) sites. In synthetic systems, trivalent RE can substitute on A-sites, with a trivalent ion, typically Al or Fe, on both octahedral and tetrahedral sites, giving the general formula $RE_3M_5O_{12}$ (M = Fe, Al, Ga). Yttrium iron garnet (YIG, $Y_3Fe_5O_{12}$) is important for magnetic, microwave, optoelectronic and imaging applications while yttrium aluminum garnet (YAG =

$Y_3Al_5O_{12}$) is an optical material and laser host, with optical properties determined by other RE dopants, *e.g.* Nd, Eu, at low concentration [8]. Thermodynamic properties of RE garnets are summarized in table 2. There is competition between garnet and perovskite phases in RE_2O_3 - M_2O_3 systems, with the garnet favored for smaller RE and the perovskite for larger. Cerium can substitute into yttrium iron garnet (YIG), and a complex balance of oxidation states (Ce^{3+}, Ce^{4+}, Fe^{2+} and Fe^{3+}) and site occupancies affects the energetics [31].

6. Phosphates and Vanadates

Rare Earth phosphates, $REPO_4$, are important as minerals and potential RE ores, as well as technological materials such as phosphors. They exist in two main structures - monazite and xenotime, determined by the RE radius. Their enthalpies of formation are highly exothermic, reflecting a strong acid-base reaction between RE_2O_3 and P_2O_5 and vary systematically with RE radius [18]. Similar trends are seen in more complex phosphates containing alkali ions as well as RE and PO_4 species [32], RE phosphates are potential laser hosts and scintillator materials. Thermodynamic trends in vanadates $REVO_4$ [33] are similar to those in phosphates $REPO_4$. Figure 6 illustrates these trends.

7. Silicates and Germanates

Thermodynamic data for RE silicate and germanate systems are included in table 3. The apatite structure is of particular interest. The parent mineral, which can exist in both hydroxide and fluoride forms, is the major ore for phosphate fertilizer but, as mentioned above, it contains significant RE and actinide impurities. Hydroxyapatite is of course an important bio-mineral for bone and tooth formation. It can also accommodate RE, and the idea of using artificially

introduced RE content for medical diagnostic and therapeutic applications is gaining ground. The energetics of RE substitution in hydroxyapatite has been determined recently [34]. In addition, apatite-structured silicates and germinates, in which the RE is a major constituent, show oxygen ion conductivity, making them potential solid electrolytes for solid oxide fuel cells (SOFC). The thermochemistry of some of these materials has been studied [35; 36; 37].

8. General Trends in Formation Enthalpies

As materials in which ionic bonding dominates, RE ternary oxides usually show a uniform trend in enthalpies of formation depending on the RE-O bond length, lattice parameter, ionic radius, or ionic potential (all of which are interrelated. These properties enable accurate interpolation and estimation of enthalpies of formation for missing RE compounds and probably for the trivalent actinides as well. However a given crystal structure can tolerate only a limited range of bond lengths. Indeed the existence of a given structure is limited by competition with other structures which become more thermodynamically favorable at smaller or larger ionic radii. This is shown schematically in figure 7, which suggests a general picture of maximum stability at a given ionic radius (or bond length), with stability decreasing in either direction away from this optimum and phase occurrence finally limited by the competition with other structures. In reality, because ionic radius cannot vary continuously but is fixed by given elements and oxidation states, one often sees only one side of this maximum and the roughly linear trends noted above. The salient point is that extrapolation is dangerous.

9. Molten, Glassy, and Amorphous Materials

Though not the major focus of this paper, the behavior of RE in molten, glassy, and amorphous oxide materials has attracted considerable attention. In general RE ions are considered "network modifiers" for silicate, borate, and phosphate melts since they do not enter tetrahedral coordination. They appear to require 7 to 10 - fold coordination and sometimes are associated with "free" or non-bridging oxygen ions, with tendencies toward clustering and phase separation [38]. Polyamorphism, the existence of amorphous (glassy) phases of identical composition but different structure and properties, with a sharp transition between them, has been studied extensively in the Y_2O_3-Al_2O_3 system (*e.g.* [39; 40]). The structure and crystallization of amorphous RE oxide powders and thin films prepared at low temperature is important for electronic applications. Some thermodynamic studies of such non - crystalline materials are listed in table 7.

10. Nanoparticles and Surface and Interface Energies

It has been shown that nanoparticles can have quite different thermodynamic properties from those of bulk phases as a consequence of their high surface areas, resulting in significant contributions of surface energy and hydration effects [26]. These can lead to crossovers in phase stability of polymorphs and major changes in equilibria involving dehydration and oxidation - reduction. Studies involving RE oxide systems are summarized in table 8.

11. Conclusions

Many new RE oxide multicomponent oxide phases have been synthesized over the past two decades in the search for optimized functional materials. Thermochemical studies are beginning to define systematic trends in stability and link energetics and properties.

Paradoxically, the thermodynamic data base for natural RE materials (minerals) is less complete than that for some of the more "popular" technological ones.

Acknowledgements

This work is supported by the Critical Materials Institute, an Energy Innovation Hub funded by the U.S. Department of Energy, Office of Energy Efficiency and Renewable Energy, Advanced Manufacturing Office.

Table 1: Rare earth minerals and other minerals which can have significant Rare Earth (RE) content. RE ores are in bold

Mineral	Mineral Chemistry
Aeschynite	$(RE,Ca,Fe,Th)(Ti,Nb)_2(O,OH)_6$
Allanite (orthite)	$(Ca,RE)_2(Al,Fe)_3(SiO_4)_3(OH)$
Anatase	TiO_2
Ancylite	$SrRE(CO_3)_2(OH)\bullet H_2O$
Apatite	**$Ca_5(PO_4)_3(F,Cl,OH)$**
Bastnasite	**$RECO_3F$**
Brannerite	$(U,Ca,RE)(Ti,Fe)_2O_6$
Britholite	$(RE,Ca)_5(SiO_4,PO_4)_3(OH,F)$
Cerite	$Ce_9(Ca)Fe^{3+},Mg)(SiO_4)_6[SiO_3(OH)](OH)_3$
Cerianite	$(Ce,Th)O_2$
Cheralite	$(RE,Ca,Th)(P,Si)O_4$
Churchite	$YPO_4\bullet 2H_2O$
Eudialyte	$Na_{15}Ca_6(Fe,Mn)_3Zr_3(Si,Nb)Si_{25}O_{73}(OH,Cl,H_2O)_5$
Euxenite	$(RE,Ca,U,Th)(Nb,Ta,Ti)_2O_6$
Fergusonite	$RE(Nb,Ti)O_4$
Florencite	$REAl_3(PO_4)_2(OH)_6$
Gadolinite	$REFeBe_2Si_2O_{10}$
Huanghoite	$BaRE(CO_3)_2F$
Hydroxylbastnasite	**$RECO_3(OH,F)$**
Kainosite	$Ca2(Y,REE)_2Si_4O_{12}CO_3\bullet H_2O$
Loparite	**$(RE,Na,Ca)(Ti,Nb)O_3$**
Monazite	**$(REE,Th)PO_4$**
Mosandrite	$(Ca,Na,RE)_{12}(Ti,Zr)_2Si_7O_{31}H_6F_4$
Parisite	$CaRE_2(CO_3)_3F_2$
Samarskite	$(RE,U,Fe)_3(Nb,Ta,Ti)_5O_{16}$
Synchisite	$CaRE(CO_3)_2F$
Thalenite	$Y_3Si_3O_{10}(OH)$
Xenotime	**YPO_4**
Yttrotantalite	$(Y,U,Fe)(Ta,Nb)O_4$
Zircon	$ZrSiO_4$

Table 2: Structure types, phase transition temperatures and enthalpies in rare earth sesquioxides.

	†t_{tr} /°C, C-B $\Delta_{tr}H$/(kJ·mol^{-1})*	B-A	A-H	B-H	C-H	H-X	t_{fus}/°C ‡ $\Delta_{fus}H$/(kJ·mol^{-1})
La_2O_3¥			2046 ±5 23 ±5			2114 ±5 17 ±5	2301 ±10 78 ±10
Ce_2O_3			(2065 ±60)			(2140 ±30)	2230
Pr_2O_3			(2080 ±50)			(2170 ±30)	2300
Nd_2O_3			2100 ±30			2200 ±10	2320 ±20
Sm_2O_3	(403 ±20) 4 ±3**[41]	1900 ±30	2130 ±30			2250 ±30	2335 ±15
Eu_2O_3	(621 ±20)	2050 ±20	2140 ±20			2270 ±20	2350
Gd_2O_3	(1152 ±20) 5.3 ±0.4[42]	2170 ±10 6 ±3[43]	2208 ±10 35 ±3 [43]			2360 ±20	2420 ±20
Tb_2O_3	1550 ±50			2167 ±20		2370 ±30	2410
Dy_2O_3	1990 ±30			2190 ±20		2380 ±40	2408
Ho_2O_3	2185 ±20			2210 ±30			2415
Y_2O_3					2327 ±30 25 ±9[44]		2439 ±12 84 ±9[44]
Er_2O_3					2320 ±50		2418
Tm_2O_3					2350 ±20		2425
Yb_2O_3					2380 ±20		2435
Lu_2O_3							2490

† Phase transition temperatures assessed by Zinkevich[45] after[46; 47; 48] values in brackets are estimates

‡ Melting temperatures are after IUPAC review[49; 50] unless noted otherwise; uncertainties indicate recommended values

¥ DTA measurements[51] temperatures are consistent with previous assessments[45; 49]

* at transition temperature, unless noted otherwise

**at 25 °C

Table 3 Thermodynamic properties of Rare Earth (RE) oxide materials.

	Thermodynamic functions for rare earth oxides						
Compound	**from elements**			**Standard entropy**	**Crystal structure**	**Method**	**Ref.**
	Enthalpy of formation $\Delta_f H^o_{298.15\ K}$ / (kJ·mol^{-1})	**Entropy of formation** $\Delta_f S^o_{298.15\ K}$ / (J·K^{-1} ·mol^{-1})	**Gibbs energy** $\Delta_f G^o_{298.15\ K}$ / (kJ·mol^{-1})	$S^o_{298.15\ K}$ / (J·K^{-1} ·mol^{-1})			
OXIDES							
Y_2O_3	**-1932.8±5.2**	*-297.5±1.0*	*-1884.1±6.2*	**99.0±0.4**	C-type	a, b	[2; 53; 54]
La_2O_3	**-1791.6±1.0**	*-294.1±2.6*	*-1705.4±3.6*	**127.3±0.9**	A-type	b, d	[55; 56]
	-1857.7		*-1770.1*		A-type	c	[57]
	-1789.0		*-1701.4*		A-type	a	[55]
	-1912.1		*-1824.5*		A-type	c	[58]
	-1907.1		*-1819.5*		A-type	c	[59]
	-2255±17		*-2167.4±19.6*		A-type	c	[60]
	-1793.1±0.8		*-2167.4±3.4*		A-type	c	[61]
	-1791.3±2.5		*-1703.7±5.1*		A-type	a	[62]
	-1794.2±2.7		*-1706.6±5.3*		A-type	a	[63]
	-1792±2.7		*-1704.4±5.3*		A-type	a	[63]
	-1794.8±2.7		*-1707.2±5.3*		A-type	a	[63]
	-1792.5±2.7		*-1707.2±5.3*		A-type	a	[63]
	-1798.2±5.2		*-1710.6±7.8*		A-type	a	[55]
	-1791.0±4.1		*-1703.4±6.7*		A-type	a	[55]
	-1791.9±6.1		*-1703.4±8.7*		A-type	a	[55]
	-1791.7±3.0		*-1703.4±5.6*		A-type	a	[55]
	-1798.2±2.4		*-1710.6±5.0*		A-type	a	[64]

	-1793.7		-1705.8	127.3	A-type	b	[65]
Ce_2O_3	**-1799.8±1.8**	*-302.6±8.9*	*-1709.6±10.7*	**148.1±0.4**	A-type	c, d	[2; 66; 67]
	-1813.0±2.0		*-1722.8±10.9*		A-type	b	[55]
	-1823.4±1.8		*-1732.5±10.7*		A-type	c	[68]
	-1790.2±1.5		*-1700.0±10.4*		A-type	c	[69]
	-1799.8±1.7		*-1709.6±10.6*		A-type	c	[66]
	-1813.1±0.8		*-1722.9±9.7*		A-type	a	[67]
	-1813.2±3.2		*-1723.0±12.1*		A-type	a	[67]
	-1809.2±5.2		*-1719.0±14.1*		A-type	a	[70]
	-1796.2		**-1706.2**	150.6	A-type	b	[65]
CeO_2	**-1090.4±0.8**	*-214.3±4.3*	*-1026.5±5.1*	**62.3±0.1**	Cubic	b, d	[2; 71; 72]
	-1088.7		-1024.7	62.3	Cubic	b	[65; 73]
Pr_2O_3	**-1809.9±3.0**	*-302.8±4.6*	-1719.73±7.6	**152.7±0.3**	A-type	a	[2; 72]
	-1831.6±3.5		-1741.4±8.1		A-type	a	[74]
	-1809.6		-1719.4		A-type	b	[65]
$PrO_{1.703}$	**-926.3±2.2**					b	[2]
$PrO_{1.717}$	**-928.4±2.6**					b	[2]
$PrO_{1.804}$	**-938.9±2.0**					b	[2]
$PrO_{1.833}$	**-944.6±2.5**			**79.9 ±2.0**		b	[2]
PrO_2	**-954.2±5.0**	*-198.2±5.2*	*-895.1±10.2*	**80.8±3.0**	Cubic	b	[2]
	-949.4		*-895.3*		Cubic	b	[65]
Nd_2O_3	**-1806.9±3.0**	*-292.4±3.6*	*-1719.8±6.6*	**158.7±1.0**	A-type	b, d	[2; 55; 56]
	-1820.0		*-1732.9*		A-type	c	[57]
	-1808.1±1.0		*-1720.9±4.6*		A-type	c	[75]

	-1798.2		*-1711.1*		A-type	c	[76]
	-1789.2		*-1702.1*		A-type	c	[76]
	-1807.1±3.1		*-1720.0±6.7*		A-type	a	[77]
	-1807.3±2.2		*-1720.25±5.8*		A-type	a	[77]
	-1799.6±4.5		*-1712.5±8.1*		A-type	a	[55]
	-1831.7±7.0		*-1744.6±10.6*		A-type	a	[78]
	-1797.1±2.1		*-1710.0±5.7*		A-type	a	[79]
	-1805.1±3.3		*-1718.0±6.9*		A-type	a	[79]
	-1807.3±4.1		*-1720.2±7.7*		A-type	a	[79]
	-1816.1±1.9		*-1729.0±5.5*		A-type	a	[80]
	-1807.9		-1720.9	158.6	A-type	b	[65]
Sm_2O_3	**-1823.0±4.0**	*-295.7*	*-1734.9*	**150.6±0.3**	B-type	b	[2]
	-1815.4±2.0		*-1734.9*		B-type	c	[81]
	-1777.3		*-1689.2*		B-type	c	[82]
	-1835.4±10.8		*-1747.3*		B-type	a	[83]
	-1831.5±5.7		*-1743.4*		B-type	a	[83]
	-1824.2±2.6		*-1736.1*		B-type	c	[41]
	-1820.8±2.9		*-1732.7*		B-type	a	[41]
	-1830.7±8.9		*-1742.6*		B-type	a	[41]
	-1824.6±7.6		*-1736.5*		B-type	a	[84]
Eu_2O_3	**-1650.4±4.0**	*-324.6±4.8*	*-15553.7±8.8*	**138.6±3.0**	B-type	b	[2; 55]
	-1648.1±3.8		*-1551.4±8.6*		B-type	c	[85]
	-1725.5±8.5		*-1628.8±13.3*		B-type	a	[55]
	-1674.0±8.9		*-1577.3±13.7*		B-type	a	[55]
	-1651.0±3.8		*-1554.3±8.6*		B-type	c	[86]
	-1652.0±6.0		*-1555.3±10.8*		B-type	a	[86]
	-1624.5±6.4		*-15527.8±11.2*		B-type	a	[86]
	-1650.7±8.0		*-1554.0±12.8*		B-type	a	[86]

	-1686.2±5.0		*-1589.5±9.8*		B-type	a	[87]
	-1730.6±5.8		*-1633.9±10.6*		B-type	a	[87]
	-1651.4		*-1554.7*		B-type	b	[65]
Eu_2O_3	**-1662.5±6.0**		*-1565.8±10.8*		C-type	b	[2]
	-1662.7		*-1566.0*		C-type	b	[65]
EuO	**-591.3±5.4**	*-96.7±1.2*	*-556.9±6.6*	**83.6±0.8**	Cubic	b	[2]
	-592.0		-556.9	62.8	Cubic	b	[65]
$EuO_{1.333}$	**-756.8±4.0**	*-438.5*	**-556.9**	**69.7±2.9**	B-type	b	[2]
Gd_2O_3	**-1819.7±3.6**	*-292.8*	-2142.2		B-type	a	[88]
	-1854 ±15			**150.9±0.15**	C-type	b	[2]
	-1782.2		-1732.4		B-type	a	[82]
	-1826.3±3.7		-1694.9		B-type	c	[55]
	-1829.5±2.6		-1739.0		B-type	c	[55]
	-1828.2±3.6		-1742.2		B-type	c	[55]
	-1819.6		-1740.9		B-type	b	[65]
Tb_2O_3	**-1865.2±6.0**	*-295.4±3.9*	-1777.2±9.9	**159.2±3.0**	C-type	b	[2; 65]
	-1864.5±8.4		-1776.5±12.3		C-type	a	[75]
$TbO_{1.510}$	**-933.4±3.6**					b	[2]
$TbO_{1.709}$	**-952.3±3.4**					b	[2]
$TbO_{1.710}$	**-953.1±3.9**					b	[2]
$TbO_{1.800}$	**-966.1±3.3**					b	[2]
$TbO_{1.817}$	**-961.9±3.5**					b	[2]
$TbO_{1.975}$	**-970.5±2.8**					b	[2]
TbO_2	**-972.1±5.0**			**86.9±3.0**	Cubic	b	[2]
Dy_2O_3	**-1863.4±5.0**	*-308.8*	-1771.4	**149.80±0.15**	C-type	b	[2]
	-1865.2±3.8		*-1773.2*		C-type	c	[89]
	-1862.9±4.2		*-1771.9*		C-type	c	[90]

	-1863.9±6.7		*-1771.9*		C-type	a	[90]
Ho_2O_3	**-1883.3±8.2**	*-300.4*	*-1793.8*	**156.38 ±0.15**	C-type	b	[2]
	-1881.0±5.0		*-1791.5*		C-type	c	[91]
	-1887.3±9.5		*-1797.8*		C-type	a	[53]
	1887.3±13.7		*-1797.8*		C-type	a	[53]
	-1900.3±15.1		*-1810.8*		C-type	a	[53]
	-1885.7±7.3		*-1796.2*		C-type	a	[53]
	-1880.7		-1791.2	**158.2**	C-type	b	[65]
Er_2O_3	**-1900.1±6.5**	*-298.2*	*-1811.2*	**153.13±0.15**	C-type	b	[2]
	-1897.8±3.8		*-1808.9*		C-type	c	[92]
	-1762.8		*-1673.9*		C-type	c	[84]
	-1898.2±4.6		*-1809.3*		C-type	a	[93]
	-1904.2±3.4		*-1815.3*		C-type	a	[53]
Tm_2O_3	**-1889.3±5.7**	*-309.8*	*-1797.0*	**139.7±0.4**	C-type	b	[2]
	-1888.7		-1794.5		C-type	b	[65]
Yb_2O_3	**-1814.5±6.0**		*-1726.8*	**133.1±0.3**	C-type	b	[2]
	-1814.6		-1726.7		C-type	b	[65]
Lu_2O_3	**-1877.0±7.7**	*-299.9*	*-1787.6*	**126.79±0.13**	C-type	b	[2]
	-1878.2		-1789.1	110.0	C-type	b	[65]
FERRITES							
$LaFeO_3$	*-1351.2±15.2*	*-246.3±21.4*	-1277.8±6.3	118.0	Perovskite	a	[13; 94]
	-1373.5±2.7	*-321.2±8.9*			Perovskite	a	[94; 95]
$PrFeO_3$	*-1364.6±16.2*	*-277.3+22.4*	-1282.0±6.3	102.7±41.9	Perovskite	a	[13; 94]
$NdFeO_3$	*-1359.9±16.2*	*-276.9±22.4*	-1277.4±6.3	116.0±21.0	Perovskite	a	[13; 96]
$SmFeO_3$	*-1367.0±16.7*	*278.3±22.9*	-1284.1±6.3	161.5±25.2	Perovskite	a	[13; 97]
$EuFeO_3$	*-1280.6±16.7*	*-288.8±22.9*	-1194.5±6.3	188.0±29.3	Perovskite	a	[13; 94]
$GdFeO_3$	*-1365.3±16.5*	*-320.3±22.7*	-1269.8±6.3	129.0±35.2	Perovskite	a	[13; 96]

$TbFeO_3$	*-1383.9±17.7*				Perovskite	a	[13]
$DyFeO_3$	*-1378.8±17.2*	*-313.7±23.4*	-1285.3±6.3	126.8±26.4	Perovskite	a	[13; 96]
$HoFeO_3$	*-1388.7±18..7*	*-334.3±24.9*	-1289.1±6.3	131.0±35.2	Perovskite	a	[13; 96]
$ErFeO_3$	*-1397.1±17.9*	*-366.7±24.1*	-1287.8±6.3	137.1±35.2	Perovskite	a	[13; 96]
$TmFeO_3$	*-1391.7±17.5*	*473.5±23.7*	-1250.6±6.3	86.0±35.2	Perovskite	a	[13; 96]
$YbFeO_3$	*-1354.3±17.7*				Perovskite	a	[13]
$LuFeO_3$	*-1385.6±18.5*				Perovskite	a	[13]
$Sm_3Fe_5O_{12}$	*-5028.4±58.3*				Garnet	a	[13; 95]
$Eu_3Fe_5O_{12}$	*-4768.9±58.3*				Garnet	a	[13; 95]
$Gd_3Fe_5O_{12}$	*-5018.2±57.7*				Garnet	a	[13; 95]
$Tb_3Fe_5O_{12}$	*-5062.4±61.3*				Garnet	a	[13; 95]
$Dy_3Fe_5O_{12}$	*-5004.6±59.8*				Garnet	a	[13; 95]
$Ho_3Fe_5O_{12}$	*-5014.4±59.8*				Garnet	a	[13; 95]
$Er_3Fe_5O_{12}$	*-4989.2±62.1*				Garnet	a	[13; 95]
$Tm_3Fe_5O_{12}$	*-4947.9±60.9*				Garnet	a	[13; 95]
$Yb_3Fe_5O_{12}$	*-4852.5±61.3*				Garnet	a	[13; 95]
$Lu_3Fe_5O_{12}$	*-4879.3±63.9*				Garnet	a	[13; 95]
ALUMINATES							
$YAlO_3$	***-1827.9±5.1***				Perovskite	a	[13]
	-1813.4±3.1				Perovskite	a	[98]
$LaAlO_3$	***-1796.8±3.7***				Perovskite	a	[13]
	-1801.6±1.5				Perovskite	a	[98]
	-1803.3±4.4				Perovskite	a	[99]
$NdAlO_3$	***-1782.7±5.6***				Perovskite	a	[13]
	-1794.1±1.8				Perovskite	a	[98]

$SmAlO_3$	***-1786.9±5.9***				Perovskite	a	[13]
	-1790.0±1.6				Perovskite	a	[98]
$EuAlO_3$	***-1693.6±5.3***				Perovskite	a	[13]
$GdAlO_3$	***-1780.0±5.4***				Perovskite	a	[13]
	-1785.0±1.8				Perovskite	a	[98]
$DyAlO_3$	***-1790.9±4.5***				Perovskite	a	[13]
	-1794.6±3.1				Perovskite	a	[98]
$Y_3Al_5O_{12}$	***-7203.9±15.0***				Garnet	a	[13]
$Dy_3Al_5O_{12}$	***-7082.0±14.1***				Garnet	a	[13]
$Ho_3Al_5O_{12}$	***-7024.2±25.5***				Garnet	a	[13]
$Er_3Al_5O_{12}$	***-7136.0±20.6***				Garnet	a	[13]
$Tm_3Al_5O_{12}$	***-7120.4±16.5***				Garnet	a	[13]
$Yb_3Al_5O_{12}$	***-6992.0±17.0***				Garnet	a	[13]
$Lu_3Al_5O_{12}$	***-7077.8±16.0***				Garnet	a	[13]
MANGANATES							
$YMnO_3$	**-1461.9±2.1**				Perovskite	a	
$LaMnO_3$	**-1451.1±2.5**				Perovskite	a	[99]
$NdMnO_3$	**-1431.9±1.8**				Perovskite	a	[99]
CHROMATES							
$LaCrO_3$	**-1536.2±5.2**				Perovskite	a	[14]
LANTHANIDES							
$BaCeO_3$	**-1686.5±3.9**				Perovskite	a	[100]
$SrCeO_3$	**-1685.6±3.8**				Perovskite	a	[100]
$BaPrO_3$	***-1639.8±21.2***				Perovskite	e	[18]
$BaTbO_3$	**-1609.0±2.7**				Perovskite	a	[100]

$SrTbO_3$	**-1612.9±2.1**				Perovskite	a	[100]
GALLATE							
$LaGaO_3$	**-1492.7±2.1**				Perovskite	a	[14]
$LaGaO_3$	**-1495.2±2.7**				Perovskite	a	[14]
SCANDATE							
$LaScO_3$	**-1888.9±2.7**				Perovskite	a	[14]
INDATES							
$LaInO_3$	**-1404.9±2.5**				Perovskite	a	[14]
PHOSPHATES							
YPO_4	**-1987.7±1.7**	*-386.8±8.7*	*-1872.4±10.5*	108.8±8.4	Xenotime	a	[101; 102]
$LaPO_4$	**-1969.7±1.9**	*-400.0±1.9*	-1850.5±1.9	108.3	Monazite	a	[103]
	-1970.7±1.8	*-403.36±1.8*			Monazite	a	[101]
$CePO_4$	**-1969.5±2.2**	*-401.3±2.2*	-1849.9±2.3	120.0	Monazite	a	[103]
	-1967.8±2.4	*-395.6±2.4*			Monazite	a	[101]
$PrPO_4$	**-1961.8±3.1**	*-402.3±3.1*	-1841.9±3.3	123.2	Monazite	a	[103]
	-1969.5±3.7	*-428.2±3.7*			Monazite	a	[101]
$NdPO_4$	**-1967.9±2.5**	*-401.0±2.5*	-1848.4±2.6	122.9	Monazite	a	[103]
	-1968.4±2.3	*-402.7±2.3*			Monazite	a	[101]
$SmPO_4$	-1965.8±2.9	*-398.7±2.9*	-1847.0±3.0	122.5	Monazite	a	[103]
	-1965.7±2.4	*-398.3±2.4*			Monazite	a	[101]
$EuPO_4$	**-1864.4±2.7**	*-412.1±2.7*	-1741.6±2.8	117.2	Monazite	a	[103]
	-1870.6±2.6	*-432.9±2.6*			Monazite	a	[101]
$GdPO_4$	**-1958.5±2.2**	*-395.0±2.2*	-1840.8±2.3	124.6	Monazite	a	[103]
$TbPO_4$	**-1971.1±4.6**	*-386.6±13.2*	*-1855.9±17.8*	138.1±12.6	Xenotime	a	[101; 102]
	-1968.6±4.6				Monazite	a	[101]

$DyPO_4$	**-1967.9±2.6**	*-388.6±13.6*	*-1852.1±16.2*	138.1±12.6	Xenotime	a	[101; 102]
$ErPO_4$	**-1976.9±2.1**	*-407.7±0.7*	-1855.4±2.1	116.6±0.1	Xenotime	a,e	[104]
	-1976.9±2.1	*-407.7±2.1*			Xenotime	a	[101]
$HoPO_4$	**-1971.6±3.4**	*-384.4±13.2*	***-1857.0±16.6***	142.3±12.6	Xenotime	a	[101; 102]
$TmPO_4$	**-1964.7±4.7**	*-387.1±13.0*	***-1849.3±17.7***	138.1±12.6	Xenotime	a	[101; 102]
$LuPO_4$	**-1955.4±4.2**	*-385.2±12.9*	***-1840.6±17.1***	117.2±12.6	Xenotime	a	[101; 102]
$YbPO_4$	**-1929.4±4.9**	*-377.1±13.2*	***-1817.0±18.1***	133.9±12.6	Monazite	a	[101; 102]
$K_3Y(PO_4)_2$	**-3998.3±7.1**				Distorted glaserite	a	[32]
$K_3Ce(PO_4)_2$	**-3996.1±8.5**				Distorted glaserite	a	[32]
$K_3Nd(PO_4)_2$	**-3975.1±6.6**				Distorted glaserite	a	[32]
$K_3Gd(PO_4)_2$	**-3979.1±9.8**				Distorted glaserite	a	[32]
$K_3Dy(PO_4)_2$	**-3988.4±7.5**				Distorted glaserite	a	[32]
$K_3Ho(PO_4)_2$	**-3993.5±7.0**				Distorted glaserite	a	[32]
$K_3Er(PO_4)_2$	**-3995.6±7.1**				Distorted glaserite	a	[32]

$K_3Lu(PO_4)_2$	**-3952.1±7.5**				Distorted glaserite	a	[32]
$Rb_3Lu(PO_4)_2$	**-3923.0±19.0**				Distorted glaserite	a	[32]
$Cs_3Lu(PO_4)_2$	**-4091.3±5.2**				Distorted glaserite	a	[32]
ZIRCONATES							
$Y_2Zr_2O_7$	***-2506.6***				Pyrochlore	f	[105]
$La_2Zr_2O_7$	-4130.4	-671.2	-3930.4	238.5	Pyrochlore	c,a	[98; 106]
	-4102.2±6.0	-576.5±6.0	*-4101±12*		Pyrochlore	a	[107]
				238.5	Pyrochlore	f,e	[105]
$Ce_2Zr_2O_7$	**-4133.8**	-706.7	-3923.2	230.2	Pyrochlore	d, a	[98; 106]
				258.5	Pyrochlore	e	[108]
				252.4	Pyrochlore	e	[103]
$Pr_2Zr_2O_7$	***-2453.1***				Pyrochlore	f	[105]
$Nd_2Zr_2O_7$	*-2443.9*				Pyrochlore	f	[105]
	-2404.6±6.6			268.6	Pyrochlore	a, e	[99; 108]
$Pm_2Zr_2O_7$				**269.5**	Pyrochlore	e	[108]
$Sm_2Zr_2O_7$	*-2455.8*				Pyrochlore	f	[105]
	-2413.4±7.6			260.4	Pyrochlore	a,e	[98; 108]
$Eu_2Zr_2O_7$	*-2256.0*			247.8±0.5	Pyrochlore	e, a	[98; 108]
$Gd_2Zr_2O_7$	*-2402.8±7.6*				Pyrochlore	a	[98]
	-2421.5			263.4±0.5	Pyrochlore	f, e	[105; 108]
TITANATES							
$Y_2Ti_2O_7$	**-3874.2±3.0**				Pyrochlore	a	[109]
La_2TiO_5	*-2848.5±6.5*				Pyrochlore	a	[110]
Nd_2TiO_5	*-2834.5±4.5*				Pyrochlore	a	[110]

Gd_2TiO_5	*-2836.3±5.8*				Pyrochlore	a	[110]
$La_2Ti_2O_7$	*-3885.0±5.8*				Pyrochlore	a	[110]
	-3855.5±3.5				Pyrochlore	a	[109]
$Nd_2Ti_2O_7$	***-3842.0***				Pyrochlore	a	[110]
$Sm_2Ti_2O_7$	**-3808.5±4.8**				Pyrochlore	a	[109]
$Eu_2Ti_2O_7$	**-3646.4±9.5**				Pyrochlore	a	[109]
$Gd_2Ti_2O_7$	**-3822.5±4.7**				Pyrochlore	a	[109; 110]
$Tb_2Ti_2O_7$	**-3851.2±9.0**				Pyrochlore	a	[109]
$Dy_2Ti_2O_7$	**-3849.2±5.5**				Pyrochlore	a	[109]
$Ho_2Ti_2O_7$	**-3848.4±6.8**				Pyrochlore	a	[109]
$Er_2Ti_2O_7$	**-3852.7±4.5**				Pyrochlore	a	[109]
$Tm_2Ti_2O_7$	**-3903.5±3.6**				Pyrochlore	a	[109]
$Yb_2Ti_2O_7$	**-3770.8±4.2**				Pyrochlore	a	[109]
$Lu_2Ti_2O_7$	**-3819.0±8.6**				Pyrochlore	a	[109]
STANNATES							
$La_2Sn_2O_7$	**-3091.0**				Pyrochlore	a	[111]
$Nd_2Sn_2O_7$	**-3060.4**				Pyrochlore	a	[111]
$Sm_2Sn_2O_7$	**-3058.8**				Pyrochlore	a	[111]
$Eu_2Sn_2O_7$	**-2889.1**				Pyrochlore	a	[111]
$Dy_2Sn_2O_7$	**-3071.9**				Pyrochlore	a	[111]
$Yb_2Sn_2O_7$	**-3007.8**				Pyrochlore	a	[111]
COBALTATES							
La_2CoO_4	***-2049.80±3.3***				Fluorite	a	[112]
$LaCoO_3$	**-1241.3±2.2**				Perovskite	a	[113]
CUPRATES							

La_2CuO_4	***-1993.0±7.3***				Fluorite	a	[112]
NICKLATE							
La_2NiO_4	***-2033.5±6.6***				Fluroite	a	[112]
$LaNiO_3$	**-1192.4±2.8**				Perovskite	a	
SILICATES							
Y_2SiO_5	**-2868.5±5.4**				Thortveitite	a	[98; 114]
$Y_{10}(SiO_4)_6N_2$	**-14145.2±16.5**				Apatite	a	[114]
$Y_2Si_2O_7$	-3854.8±6.8				Pyrochlore	a	[115]
	-3820.5±6.7					a	[98]
β-$La_2Si_2O_7$	-3815.7±4.5	-658.4	-3619.5	210.3	Pyrochlore C-type	a,d	[116; 117]
	-3807.6±4.5	-675.2	-3606.2	220.3		a,d	[116; 117]
$Pr_2Si_2O_7$				**272.3**	Pyrochlore	e	[108]
$Dy_2Si_2O_7$	**-3776.1±4.6**				Pyrochlore	a	[115]
Yb_2SiO_5	**-2774.8±8.3**				Thortveitite	a	[114]
	-2774.8±8.4					a	[98]
SUPERCONDUCTORS							
$PrBa_2Cu_3O_{7-\delta}$	**-2610.8±13.1**				Layered perovskite	a	[118]
$NdBa_2Cu_3O_{7-\delta}$	**-2613.9±8.0**				Layered perovskite	a	[118]
	-2661.5±14.3				Layered perovskite	a	[119]
$EuBa_2Cu_3O_{7-\delta}$	**-2528.2±8.4**				Layered perovskite	a	[118]
$GdBa_2Cu_3O_{7-\delta}$	**-2609.4±7.7**				Layered perovskite	a	[118]
	-2652.9±13.1				Layered perovskite	a	[119]

$DyBa_2Cu_3O_{7-\delta}$	**-2623.3±7.7**				Layered perovskite	a	[118]
$HoBa_2Cu_3O_{7-\delta}$	**-2637.6±8.4**				Layered perovskite	a	[118]
	-2666.1±16.7				Layered perovskite	a	[119]
$TmBa_2Cu_3O_{7-\delta}$	**-2635.8±7.5**				Layered perovskite	a	[118]
$YBa_2Cu_3O_{7-\delta}$	**-2657.5±7.5**				Layered perovskite	a	[118]
					Layered perovskite	a	[119]
$SmBa_2Cu_4O_8$	**-2827.6±8.5**				Layered perovskite	a	[118]
$EuBa_2Cu_4O_8$	**-2735.3±9.4**				Layered perovskite	a	[118]
$GdBa_2Cu_4O_8$	**-2803.0±8.7**				Layered perovskite	a	[118]
$DyBa_2Cu_4O_8$	**-2833.1±8.7**				Layered perovskite	a	[118]
$HoBa_2Cu_4O_8$	**-2853.2±9.8**				Layered perovskite	a	[118]
$Y_2Cu_2O_5$	**-2209.0±4.0**				Layered perovskite	a	[120]
Y_2BaCuO_5	**-2660.0±4.0**				Layered perovskite	a	[120]
VANADATES							
YVO_4	**-1839.2±1.9**				Tetragonal zircon	a	[33]
$CeVO_4$	**-1875.0±3.0**				Tetragonal zircon	a	[33]

$PrVO_4$	**-1803.6±1.8**				Tetragonal zircon	a	[33]
$NdVO_4$	**-1806.8±2.3**				Tetragonal zircon	a	[33]
$SmVO_4$	**-1802.2±2.3**				Tetragonal zircon	a	[33]
$EuVO_4$	**-1712.2±2.2**				Tetragonal zircon	a	[33]
$GdVO_4$	**-1797.5±1.6**				Tetragonal zircon	a	[33]
$TbVO_4$	**-1811.9±2.1**				Tetragonal zircon	a	[33]
$DyVO_4$	**-1780.8±2.1**				Tetragonal zircon	a	[33]
$HoVO_4$	**-1824.6±1.9**				Tetragonal zircon	a	[33]
$ErVO_4$	**-1797.5±3.2**				Tetragonal zircon	a	[33]
$TmVO_4$	**-1810.9±2.3**				Tetragonal zircon	a	[33]
$LuVO_4$	**-1799.9±2.3**				Tetragonal zircon	a	[33]
CARBONATES							
$La_2(CO_3)_3$	**-3213.3**		-3141.8			b	[65]
$Pr_2(CO_3)_3$						b	[65]
$Nd_2(CO_3)_3$			-3115.0			b	[65]
$Sm_2(CO_3)_3$			-3102.0			b	[65]

$Tb_2(CO_3)_3$	**-3329.2**					b	[65]
$La_2O_2CO_3$ II	***-2388.4±3.5***	*-864.3±61.0*	*-2630.8±63.5*	*170.8±2.3*		a	[121] [122]
$Nd_2O_2CO_3$ II	***-2382.1±9.4***	*-618.7*±5.0	*-2197.7±14.4*	*195.376±2.4*		a	[121] [122]
$Eu_2O_2CO_3$ II	**-2202.4±12.0**					a	[121]
$EuCO_3$			-1115.5		Rhombohedral	g	[123]
HYDROXIDES							
$Y(OH)_3$	**-1472.3±10.0**	*-449.0±10.0*	-1338.5±10.0	99.2	Cubic	b, a	[124; 125]
$La(OH)_3$	-1416.7±1.3	*-444.6±1.3*			Cubic	a	[126]
	-1415.5±1.4	*-440.6±1.4*				a	[127]
	-1416.1	*-442.6*	-1284.2±1.3	117.8		b, a, d	[128]
	-1410.1±3.3	*-422.5±3.3*				a	[129]
	-1415.5±1.4	*-440.6±1.4*				a	[127]
	-1416.7±1.3	*-444.6±1.3*				a	[126]
	-1410.01	*-422.2*				b	[127]
LaOOH	**-1078.6±1.4**	*-368.9±10.0*	*-968.7±11.4*	83.7±8.4	Cubic	a	[127]
$Ce(OH)_3$	**-1418.6±10.0**	*-443.6±10.0*	-1286.4±10.0	129.4±1.0	Cubic	b	[124]
$Pr(OH)_3$	**-1404.0**	*-399.6*	-1284.9	131.7	Cubic	a, b,d	[65; 129; 130]
	-1409.7±4.9	*-418.8±4.9*				a	[53]
	-1413.8±10	*-432.5±10.0*	-1280.9±10.0			b	[124]
$Nd(OH)_3$	-1403.7±1.0	-445.30±0.20	-1270.9±1.1		Cubic	a	[78]
	-1415.6±2.3	*-445.0±2.3*	-1283.0±2.6	129.9		a, b,d	[124; 126; 131]
	-1403.8±1.0	*-405.4±1.0*				a	[78]
	-1404.2±3.3	*-406.7±3.3*				a	[126]

	-1415.6±2.3	*-445.0±2.3*				a	[126]
$Sm(OH)_3$	**-1406.6±2.2**	*-447.3±2.2*	-1273.3±2.3	125.8±1.0	Cubic	a, b	[127]
	-1425.1±5.2	*-509.4±5.2*				a	[53]
$Eu(OH)_3$	**-1319.1±10.0**	*-464.8±20*	**-1180.6±10.0**	119.9	Cubic	b, d	[124; 132]
			-1194.5			b	[65]
$Gd(OH)_3$	**-1408.9±10.0**	*-445.3±10.0*	-1276.2±10.0	126.6	Cubic	b, d	[124; 132]
$Tb(OH)_3$	**-1414.8±10.0**	*-448.7±10.0*	-1281.1±10.0	128.4	Cubic	b, a	[124; 131]
$Dy(OH)_3$	**-1428.4±10.0**	*-448.3±10.0*	-1294.8±10.0	130.3±1.0	Cubic	b	[124]
$Ho(OH)_3$	**-1431.1±10.0**	*-448.7±10.0*	-1297.4±10.0	130.0	Cubic	b, d	[124]
$Er(OH)_3$	**-1432.5±10.0**	*-448.3±10.0*	-1298.9±10.0	128.6±1.0	Cubic	b	[124]
	-1425.6	*-425.2*	*-1298.89*	*151.3*		b	[133]
$Tm(OH)_3$	**-1421.1±10.0**	*-451.3±10.0*	-1286.6±10.0	126.5±1.0	Cubic	b	[124]
$Yb(OH)_3$	**-1395.5±11.0**	*-445.0±11.0*	-1262.9±11.0	118.6±2.0	Cubic	b	[124]
INTERLANTHANIDES							
$LaHoO_3$	*-1845.8±8.0*				Perovskite	a	[10]
$LaErO_3$	*-1855.8±6.9*				Perovskite	a	[10]
$LaTmO_3$	*-1851.3±6.2*				Perovskite	a	[10]
$LaYbO_3$	*-1815.4±6.5*				Perovskite	a	[10]

Table 4. Thermochemical studies of ionic substitutions in perovskite, K_2NiF_4 and fluorite structures

System	Reference
Perovskite	
$La_{1-x}A_xCrO_{3-\delta}$ (A = Ca, Sr)	Cheng and Navrotsky 2005[134]
$La_{1-x}Sr_xFeO_{3-\delta}$	Cheng *et al.* 2005[135]
$La_{6.7}Sr_{0.3}Mn_{1-x}Fe_xO_3$	Kemik *et al.* 2011[136]
$La_{1-x}A_xGa_{1-y}Mg_yO_3$ (A = Br, Ba)	Cheng and Navrotsky 2004[137]
Y substituted ATO_3 (A= Ca, Sr, Ba)	Navi *et al.* 2011[138]
K_2NiF_4	
$La_{2-x}Sr_xCuO_{4-\delta}$	Bularzik *et al.* 1990[139], 1991[140]
$La_{2-x}A_xCuO_{4-\delta}$ (A = Ba,Sr,Ca,Pb)	DiCarlo *et al.* 1992[141]
$La_{2-x}A_xNiO_{4-\delta}$ (A = Ba,Sr)	DiCarlo *et al.* 1993[142]
$La_{2-x}Sr_xCoO_{4-\delta}$	Prasanna *et al.* 1994[143]
Fluorite	
$Ce_{1-x}(Nd,Sm)_xO_{2.0-0.5x}$	Buyukkilic *et al.* 2012[144], 2014[145]
$Ce_{1-x}Y_xO_{2.0-0.5x}$	Chen *et al.* 2005[146]
$Ce_{1-x}M_xO_{2.0-0.5x}$ (M = La, Gd, Y)	Chen *et al.* 2006[147]
$xCe_{0.8}Y_{0.2}O_{1.9}$-$(1-x)Zr_{0.8}Y_{0.2}O_{1.9}$	Chen *et al.* 2007[148]
$Zr_{1-x}Y_xO_{2.0-0.5x}$	Lee *et al.* 2003[149]
$Hf_{1-x}Y_xO_{2.0-0.5x}$	Lee and Navrotsky 2004[150]
CeO_2-ZrO_2	Lee *et al.* 2008[151]
$A_xBi_{1-x}O_{1.5}$ (A = Dy,Yb)	Tran and Navrotsky 2012[152], 2014[153]
$Zr_{1-x}A_xO_{2.0-0.5x}$ (A = Sm, Gd, Dy, Yb, Sc)	Simoncic and Navrotsky 2007[27]
$Hf_{1-x}A_xO_{2.0-0.5x}$ (A = Sm, Gd, Dy, Yb)	Simoncic and Navrotsky 2007[28]
$Th_{1-x}A_xO_{2.0-0.5x}$ (A = La, Y)	Aizenshtein *et al.* 2010[154]
ThO_2-CeO_2	Shvareva *et al.* 2011[155]

Table 5: Charge coupled substitutions involving Rare Earth (RE) elements and Nb (or Ta) in perovskite and pyrochlore mineral systems

Perovskite

Name	Composition	Charge coupled substitution
Perovskite	$CaTiO_3$	None
Loparite	$Na_{0.5}Ce_{0.5}TiO_3$	$Ca^{2+} = 0.5\ Na^{+} + 0.5\ Ce^{3+}$ (or other large RE)
Lueshite	$NaNbO_3$	$Ca^{2+} + Ti^{4+} = Na^{+} + Nb^{5+}$
Latrappite	$CaFe_{0.5}Nb_{0.5}O_3$	$Ti^{4+} = 0.5\ Fe^{3+} + 0.5\ Nb^{5+}$
Tausonite	$SrTiO_3$	$Ca^{2+} = Sr^{2+}$
Synthetic	$REAlO_3$	$Ca^{2+} + Ti^{4+} = RE^{3+} + Al^{3+}$
Synthetic	$REFeO_3$	$Ca^{2+} + Ti^{4+} = RE^{3+} + Fe^{3+}$
Synthetic	$RE_2Ti_2O_7$	$Ca^{2+} = RE^{3+} + 0.5\ O^{2-}$ (in extra layer)
Synthetic	Ca_2Nb_2 (or Ta_2)O_7	$Ti^{4+} = Nb^{5+}$ (or $Ta^{5+)}$ + 0.5 O^{2-} (in extra layer)

Pyrochlore

Series	Substitution
$RE_2Ti_2O_7$ - $Ca_2Nb_2O_7$	$RE^{3+}{}_A + Ti^{4+}{}_B = Ca^{2+}{}_A + Nb^{5+}{}_B$
$RE_2Ti_2O_7$ - $RE_2RE'NbO_7$	$2Ti^{4+}{}_B = RE'^{3+}{}_B + Nb^{5+}{}_B$
$Ca_2Nb_2O_7$ - $CaNaNb_2O_6F$	$Ca^{2+}{}_A + O^{2-}{}_Y = Na^{+}{}_A + F^{-}{}_Y$
$CaNaNb_2O_6F$ - $CaNaNb_2O_6OH$	$F^{-}{}_Y = OH^{-}{}_Y$

Table 6. Thermochemical studies of pyrochlore – fluorite – transformations. RE denotes rare earth element.

System	Reference
$RE_2Sn_2O_7$	Lian *et al.* 2006[111]
$RE_2Ti_2O_7$	Helean *et al.* 2004[109]
HfO_2-La_2O_3-$Gd2O_3$	Ushakov *et al.* 2009[156]
$Eu_2Zr_2O_7$	Saradhi *et al.* 2012[157]
$RE_2Ti_2O_7$	Hayun *et al.* 2012[158]
$La_2Zr_2O_7$	Hong *et al.* 2014[159]

Table 7 Thermodynamic studies for molten, glassy, and amorphous Rare Earth (RE) oxide systems

System	Properties	Reference
NiO, CuO, La_2O_3, TiO_2, HfO_2 in sodium silicate liquids	Enthalpy of solution	Wilding and Navrotsky 2000[160], Linard *et al.* 2008[161]
Gd_2O_3 –in sodium aluminoborosilicate glass	Enthalpy of solution	Zhang *et al.* 2008[162]
RE_2O_3-Al_2O_3 glasses	Polyamorphism thermodynamics	Wilding *et al.* 2002 [39; 40]
$2NdAlO_3$-$3SiO_2$ glasses	Formation enthalpy	Zhang *et al.* 2003[163]
Re-Si-Al-O-N glasses	Oxidation enthalpy	Zhang and Navrotsky 2003[164]
Y_2O_3-Al_2O_3-SiO_2 glasses	Oxidation enthalpy	Zhang and Navrotsky 2003[165]
La and Y in amorphous HfO_2 and ZrO_2	Effect on crystallization	Ushakov *et al.* 2004[166; 167]
La_2O_3-HfO_2-SiO_2 glasses	Formation enthalpy	Morcos *et al.* 2008[168]
$SrTiSiO_5Y_2O_3$ glasses	Formation enthalpies	Park *et al.* 2009[169]
$Sr_2TiSi_2O_8$-Y_2O_3	Formation and crystallization enthalpies	Park *et al.* 2010[170]

Table 8 Thermochemical studies of rare earth oxide nanoparticles and their surface and interface energies

System	Properties	Reference
Y_2O_3	Surface energy, polymorphism	Zhang and Navrotsky 2008[171]
Yttria stabilized zirconia	Interface and surface energy	Chen *et al.* 2009[172], 2011[173]
CeO_2	Interface and surface energy	Hayun *et al.*, 2011[174; 175]
Yttria stabilized hafnia	Surface energy	Zhou *et al.* 2012[176]
$LaMnO_{3-\delta}$ perovskite	Surface energy	Vradman and Navrotsky 2013[177]

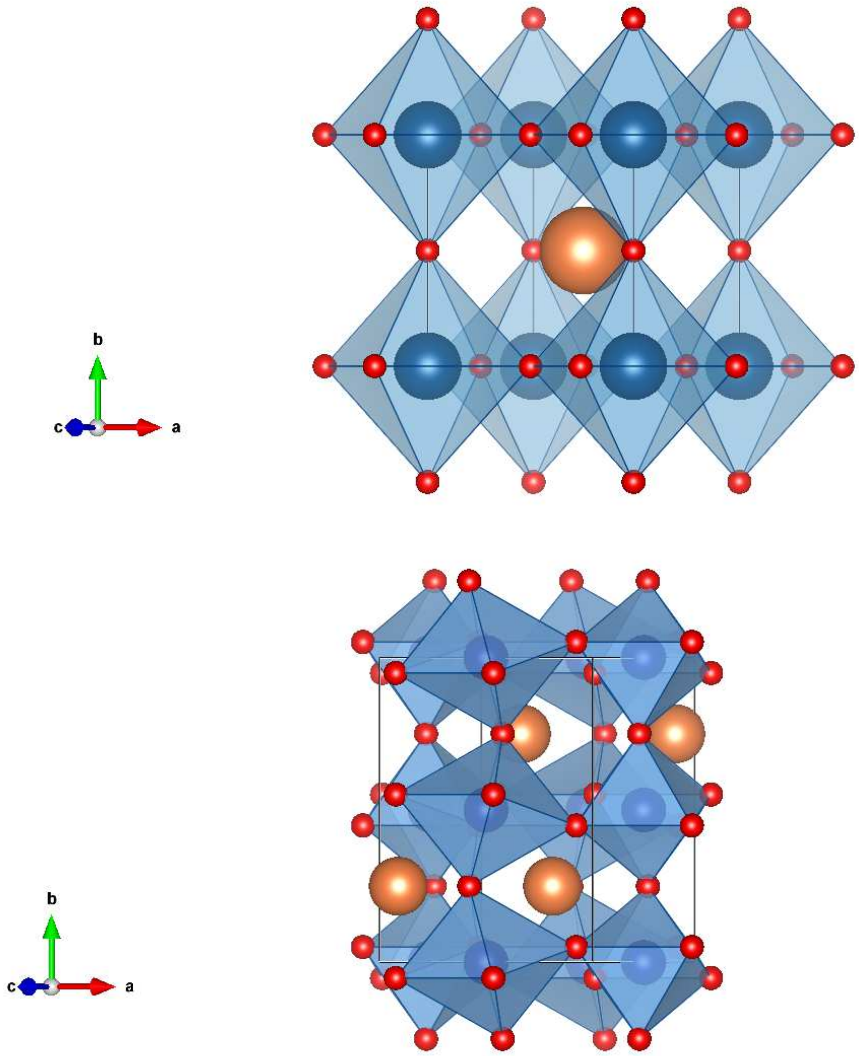

Figure. 1. Perovskite structure. Top: ideal cubic structure/ Bottom: Orthorhomibic distortion, showing enough octahedral to illustrate pattern of rotations.

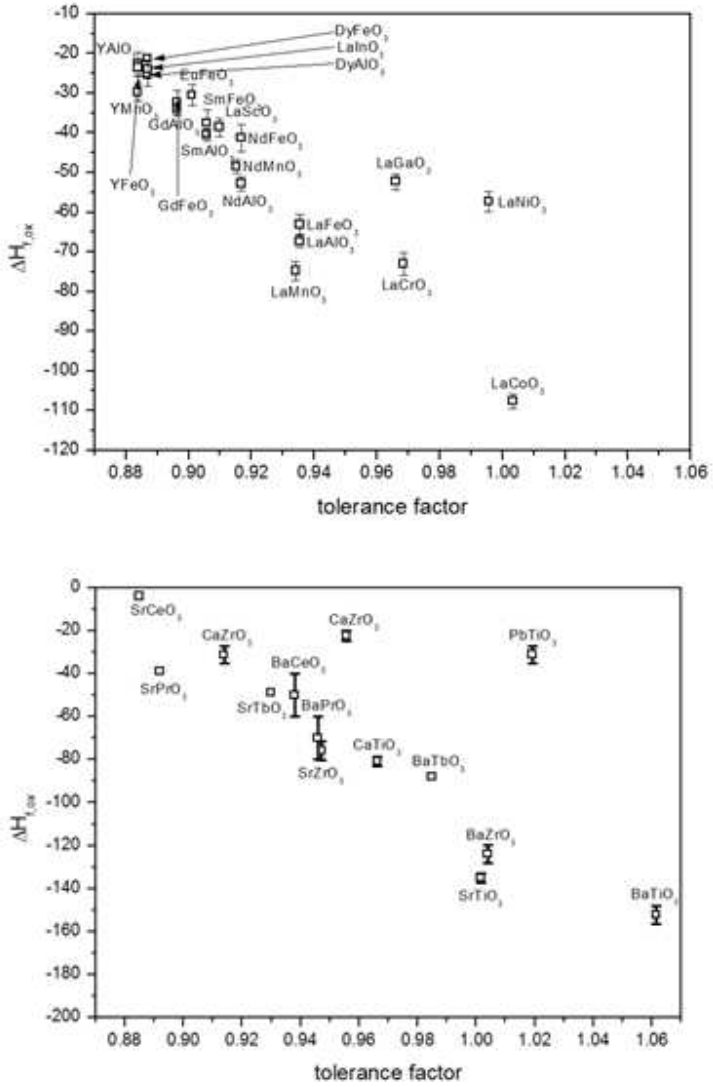

Figure. 2. Enthalpy of formation as $\Delta_f H^o_{298.15\,K}$ /(kJ·mol^{-1}) from binary oxides versus tolerance factor for (a) 3-3 perovskites [13; 14; 95; 113; 178], ionic radii for eight-fold coordination after Shannon [179] and (b) 2-4 perovskites [11; 18], ionic radii for twelve-fold coordination after Shannon [179].

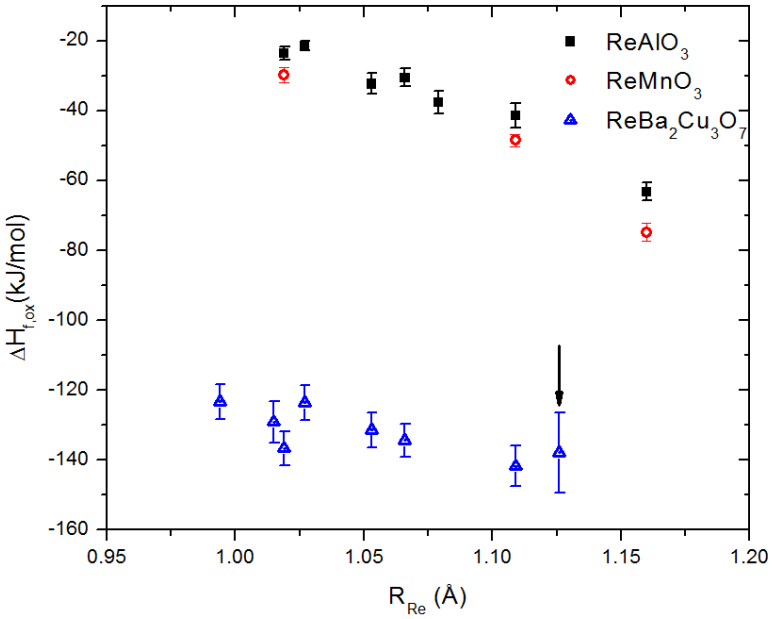

Figure 3. Enthalpy of formation as $\Delta_f H^o_{298.15\ K}$ /(kJ·mol^{-1}) for binary oxides of perovskites versus ionic radius r as 10r/nm [14; 99; 118]. Ionic radii for eight-fold coordination after Shannon [179]. Arrow marks $PrBa_2Cu_3O_{7.}$ Rare Earth elements are denoted RE.

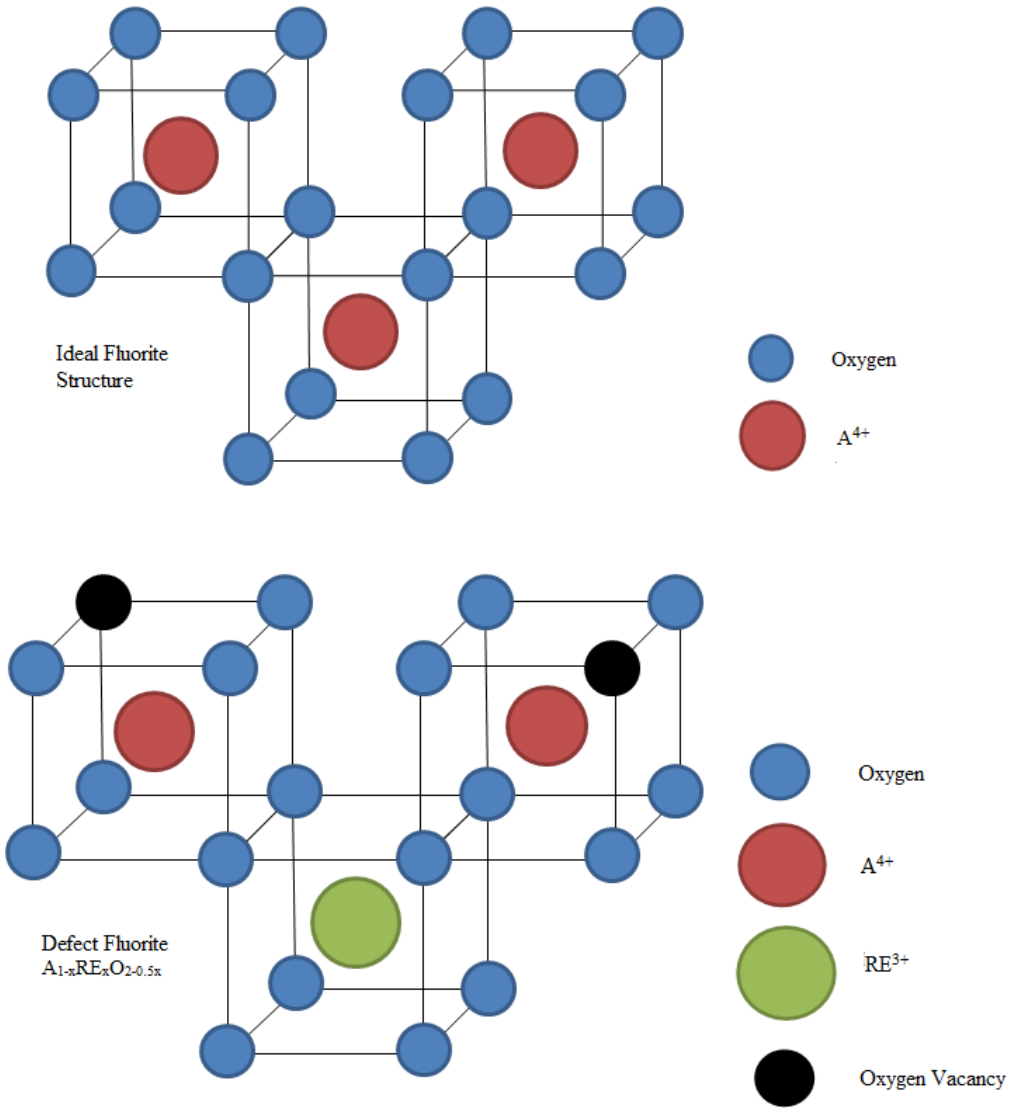

Figure 4. The fluorite structure. Top shows the perfect AO_2 structure and bottom shows a defect fluorite $A_{1-x}RE_xO_{2-0.5x}$, indicating altervalent cations and oxygen vacancies. $^{3+}$

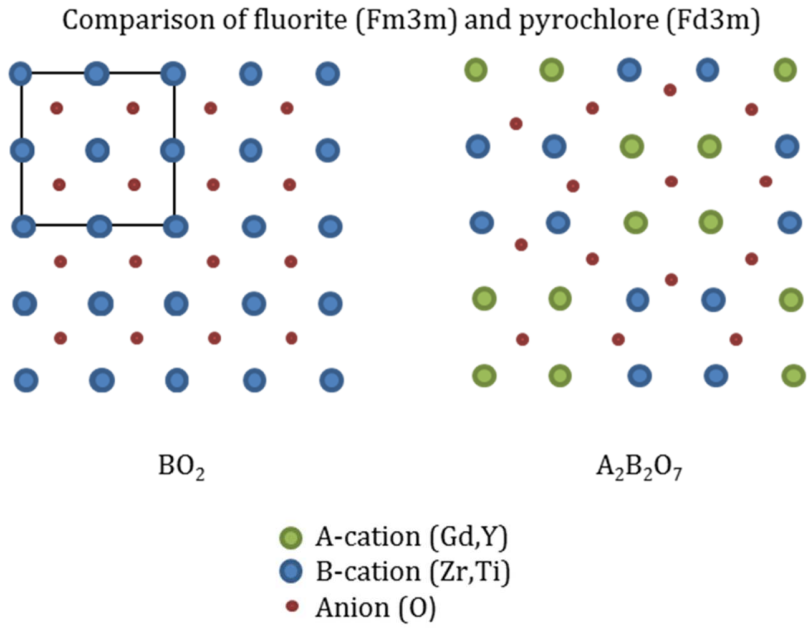

Figure 5. Schematic diagram comparing the fluorite and pyrochlore structures to show cation ordering and anion displacement**.** After [180].

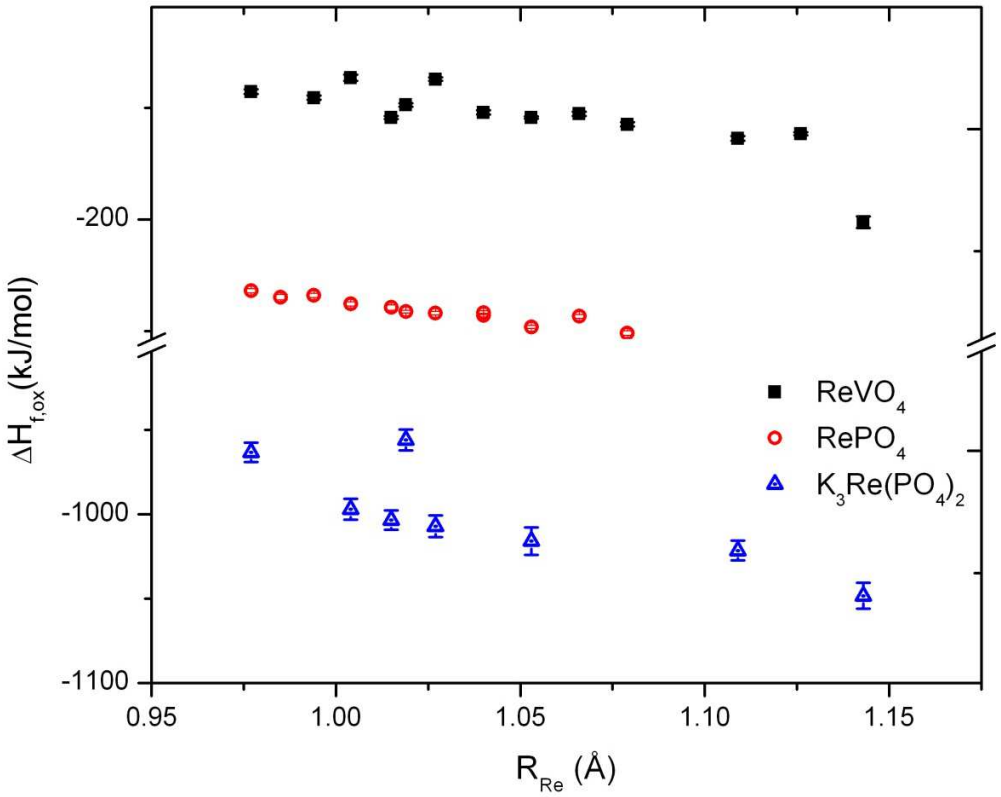

Figure 6. Enthalpies of formation $\Delta_f H^o_{298.15\ K}$ /(kJ·mol^{-1}) for Rare Earth (RE) oxides, phosphates and vanadates versus ionic radius as 10*r*/nm [32; 33; 181]. Ionic radii for eight-fold coordination after Shannon [179].

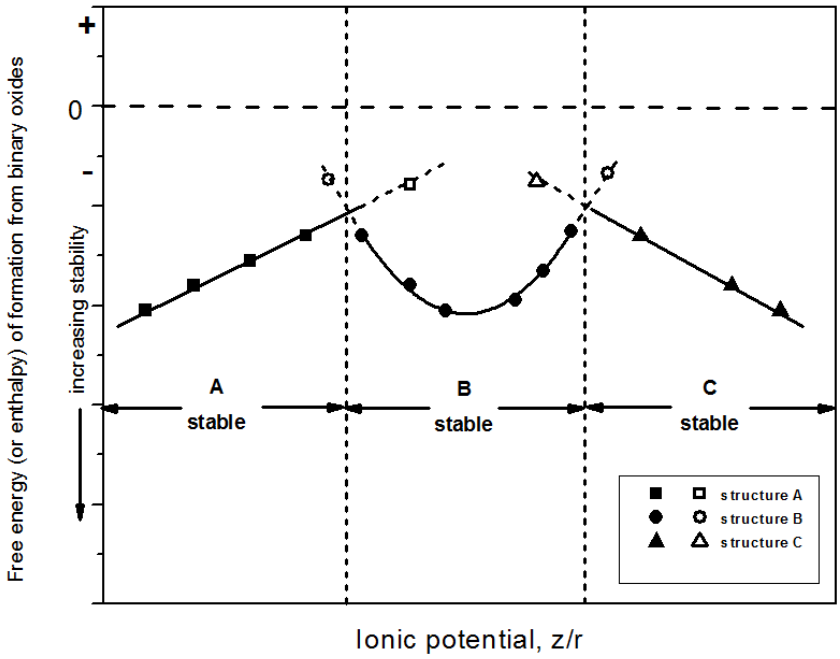

Figure 7. Schematic representation of the Gibbs energy (or enthalpy of formation from binary oxides of a set of ternary compounds or phase assemblages, each of constant composition, as the ionic potential of one cation (*e.g.*, trivalent or tetravalent lanthanide or actinide) is varied. [182]

REFERENCES

[1] G.-Y. Adachi, N. Imanaka, Chemical Reviews 98 (1998) 1479-1514.

[2] L.R. Morss, & Konings, R. J. M., Thermochemistry of Binary Rare Earth Oxides. in: G. Adachi, Imanaka, N., & Kang, Z. C. , (Ed.), Binary Rare Earth Oxides, Kluwer Academic, Dordrecht, The Netherlands, 2004, pp. 163-188.

[3] Z.C. Kang, L. Eyring, Journal of Alloys and Compounds 249 (1997) 206-212.

[4] H. Inaba, A. Navrotsky, L. Eyring, Journal of Solid State Chemistry 37 (1981) 67-76.

[5] H. Inaba, A. Navrotsky, L. Eyring, Journal of Solid State Chemistry 37 (1981) 77-84.

[6] S.A. Gramsch, Morss, L. R., Journal of Chemical Thermodynamics 27 (1995) 551-560.

[7] A. Gour, S. Singh, R.K. Singh, M. Singh, Pramana - J Phys 71 (2008) 181-186.

[8] V.B. Kravchenko, Y.L. Kopylov, Oxide Laser Ceramics. in: B. Denker, E. Shklovsky, (Eds.), Handbook of Solid-State Lasers, Woodhead Publishing, 2013.

[9] A. Navrotsky, Pure Appl Chem 66 (1994) 1759-1764.

[10] J. Qi, Guo, X., Mielewczyk-Gryn, A., and Navrotsky, A., Journal of Solid State Chemistry (Submitted 2015).

[11] E. Takayama-Muromachi, A. Navrotsky, Journal of Solid State Chemistry 72 (1988) 244-256.

[12] A. Navrotsky, Thermochemistry of Perovskites. in: A. Navrotsky, D.B. Weidner, (Eds.), Perovskite - A Structure of Great Interest to Geophysics and Materials Science, American Geophysical Union, Washington D. C., USA 1989, pp. 67-80.

[13] Y. Kanke, A. Navrotsky, Journal of Solid State Chemistry 141 (1998) 424-436.

[14] J. Cheng, A. Navrotsky, Journal of Materials Research 18 (2003) 2501-2508.

[15] J. Cheng, A. Navrotsky, Journal of Solid State Chemistry 20 (2005) 191-200.

[16] A. Navrotsky, Thermochemistry of Complex Perovskites. in: R.E. Cohen, (Ed.), Fundamental Physics of Ferroelectrics 2000: Aspen Center for Physics Winter Workshop, American Institute of Physics, 2000, pp. 288-296.

[17] A. Navrotsky, Electrochemical Society Transactions 45 (2012) 11-17.

[18] S.V. Ushakov, J. Cheng, A. Navrotsky, J.R. Wu, S.M. Haile, Materials Research Society Symposium Proceedings 718 (2002) 71-76.

[19] N.L. Allan, W.C. Mackrodt, High-Tc (sub) Superconductors. in: C.R.A. Catlow, (Ed.), Computer Modelling in Inorganic Crystallography, Academic Press, London, U. K., 1997.

[20] P. Karen, A. Kjekshus, Phase Diagrams and Thermodynamic Properties. in: K.A.G. Jr., L. Eyring, M.B. Maple, (Eds.), Handbook on the Physics and Chemistry of Rare Earths: High Temperature Rare Earths Supercoundtors-I, Elsevier, 2000, pp. 229-373.

[21] M.E. Parks, A. Navrotsky, K. Mocala, E. Takayama-Muromachi, A. Jacobson, P.K. Davies, Journal of Solid State Chemistry 79 (1989) 53-62.

[22] Z. Zhou, A. Navrotsky, Journal of Materials Research 8 (1993) 3023-3031.

[23] A. Mehta, J. DiCarlo, A. Navrotsky, Journal of Solid State Chemistry 101 (1992) 173-185.

[24] V.E. Lamberti, M.A. Rodriguez, J.D. Trybulski, A. Navrotsky, Journal of Materials Research 11 (1996) 1061-1064.

[25] A. Navrotsky, Journal of Materials Chemistry 15 (2005) 1883-1890.

[26] A. Navrotsky, Journal of Materials Chemistry 20 (2010) 10577-10587.

[27] P. Simoncic, A. Navrotsky, Journal of the American Ceramic Society 90 (2007) 2143-2150.

[28] P. Simoncic, A. Navrotsky, Journal of Materials Research 22 (2007) 876-885.

[29] J.S. Gardner, M.J.P. Gingras, J.E. Greedan, Reviews of Modern Physics 82 (2010) 53-107.

[30] J. Lian, J.W. Weber, W. Jiang, L.M. Wang, L.A. Boatner, R.C. Ewing, Nuclear Instruments & Methods in Physics Research, Section B: Beam Interactions with Materials and Atoms 250 (2006) 128-136.

[31] X. Guo, A.H. Tavakoli, S. Sutton, R. Kukkadapu, A. Lanzirotti, M. Newville, M. Asta, A. Navrotsky, Chemistry of Materials 26 (2014) 1133-1143.

[32] S.V. Ushakov, Navrotsky, A., Farmer, J. M., & Boatner, L. A., Journal of Materials Research 19 (2004) 2165-2175.

[33] M. Dorogova, A. Navrotsky, L.A. Boatner, Journal of Solid State Chemistry 180 (2007) 847-851.

[34] S.M. Hosseini, C. Drouet, A. Al-Kattan, A. Navrotsky, American Mineralogist In Press (2014).

[35] A.S. Risbud, K.B. Helean, M.C. Wilding, P. Lu, A. Navrotsky, Journal of Materials Research 16 (2001) 2780-2783.

[36] S.M. Hosseini, T. Shvareva, A. Navrotsky, Solid State Ionics 233 (2013) 62-66.

[37] S.M. Hosseini, A. Navrotsky, Journal of the American Ceramic Society 96 (2013) 3915-3919.

[38] M.C. Wilding, Y. Badyal, A. Navrotsky, Journal of Non-Crystalline Solids 353 (2007) 4792-4800.

[39] M.C. Wilding, P.F. McMillan, A. Navrotsky, Physics and Chemistry of Glasses 43 (2002) 306-312.

[40] M.C. Wilding, P.F. McMillan, A. Navrotsky, Physica A 314 (2002) 379-390.

[41] F.B. Baker, G.C. Fitzgibbon, D. Pavone, C.E.H. Jr., L.D. Hansen, E.A. Lewis, Journal of Chemical Thermodynamics 4 (1972) 621-636.

[42] U. Kolitsch, Hochtemperaturkalorimetrie und Phasenanalytik in SE2O3–Al2O3–SiO2–Systemen, University of Stuttgart, 1995, pp. 242.

[43] L.S. Barkhatov, L.I. Zhmakin, D.N. Kagan, V.V. Koroleva, E.E. Shpil'rain, High Temperatures- High Pressures, European Thermophysical Properties Conference, Antwerp, Belgium 13 (1981) 39-42.

[44] E.E. Shpil'rain, D.N. Kagan, L.S. Barkhatov, V.V. Koroleva, J.P. Coutures, M. Foex, Rev. Int. Hautes Temp. Refract. 15 (1979) 249-252.

[45] M. Zinkevich, Progress in Materials Science 52 (2007) 597-647.

[46] M. Foex, J.P. Traverse, Rev. Int. Hautes Temp. Refract. 3 (1966) 429-453.

[47] J. Coutures, A. Rouanet, R. Verges, M. Foex, J. Solid State Chem. 17 (1976) 171-182.

[48] A.V. Shevchenko, L.M. Lopato, Pure Appl Chem 61 (1985) 1461-1482.

[49] J.P. Coutures, M.H. Rand, Pure Appl Chem 61 (1989) 1461-1482.

[50] J. Hlavac, Pure Appl Chem 54 (1982) 681-688.

[51] S.V. Ushakov, A. Navrotsky, Journal of Materials Research 26 (2011) 845-847.

[52] V.M. Goldschmidt, F. Ulrich, T. Barth, Skrifter utgit av det norske Videnskap-Akademii Oslo. (I) Matem.-Naturvid. Klasse 5 (1925) 5-24.

[53] L.R. Morss, P.P. Day, C. Felinto, H. Brito, The Journal of Chemical Thermodynamics 25 (1993) 415-422.

[54] G.V.E. Gavrichev K.S. , Golushina L.N., Nikiforova G.E., Totrova G.A, and Shaplygin I.S. , Russian Journal of Physical Chemistry 67 (1993) 1554.

[55] E.H.P. Cordfunke, R.J.M. Konings, Thermochimica acta 375 (2001) 65-79.

[56] B.H. Justice, E.F. Westrum, The Journal of Physical Chemistry 67 (1963) 339-345.

[57] W. Muthmann, L. Weiss, European Journal of Organic Chemistry 331 (1904) 1-46.

[58] H.C. Kremers, R.G. Stevens, Journal of the American Chemical Society 45 (1923) 614-617.

[59] J.E. Moose, S.W. Parr, Journal of the American Chemical Society 46 (1924) 2656-2661.

[60] W.A. Roth, V. Wolf, O. Fritz, Zeitschrift für Elektrochemie 46 (1940) 42-45.

[61] E.J. Huber, C.E. Holley, Journal of the American Chemical Society 75 (1953) 5645-5647.

[62] R.L. Montgomery, Hubert, T.D., Thermochemistry of Samarium, U.S. Department of the Interior, Bureau of Mines, Washington, 1959.

[63] G.C. Fitzgibbon, C.E. Holley, Jr., I. Wadso, Journal of Physical Chemistry 69 (1965) 2464-2466.

[64] H. Oppermann, Morgenstern, A., Ehrlich, S., Zeitschrift für Naturforschung B 52 (1997) 1062–1066.

[65] R.H. Schumm, Wagman, D. D., Bailey, S., Evans, W. H., & Parker, V. B . , Selected Values of Chemical Thermodynamic properties. Tables for the Lanthanide (Rare Earth) Elements (Elements 62 thorugh 76 in the Standard Order of Arrangement), National Bureau of Standards, National Bureau of Standards, 1973.

[66] F.B. Baker, C.E. Holley, Journal of Chemical & Engineering Data 13 (1968) 405-407.

[67] M.E. Huntelaar, A.S. Booij, E.H.P. Cordfunke, R.R. van der Laan, A.C.G. van Genderen, J.C. van Miltenburg, The Journal of Chemical Thermodynamics 32 (2000) 465-482.

[68] F.A. Kuznetsov, T.N. Rezukhina, A.N. Golubenko, Russian Journal of Physical Chemistry 34 (1960) 1010-1011.

[69] A.D. Mah, Heats of Formation of Cerium Sesquioxide and Bismuth Sesquioxide by Combustion Calorimetry, Technical Report USBM-RI-5676, U.S. Bureau of Mines, 1961.

[70] R.L. Putnam, A. Navrotsky, E.H.P. Cordfunke, M.E. Huntelaar, Journal of Chemical Thermodynamics 32 (2000) 911-921.

[71] B.H. Justice, E.F. Westrum, The Journal of Physical Chemistry 73 (1969) 1959-1962.

[72] G.C. Fitzgibbon, E.J.J. Huber, C.E. Holley, Jr., Rev. Chim. Miner. 10 (1973) 1973.

[73] J.B. Gruber, B.H. Justice, J.E.F. Westrum, B. Zandi, The Journal of Chemical Thermodynamics 34 (2002) 457-473.

[74] C.T. Stubblefield, H. Eick, L. Eyring, Journal of the American Chemical Society 78 (1956) 3877-3879.

[75] E.J.J. Huber, C.E. Holley, Jr., Journal of the American Chemical Society 74 (1952) 5530-5531.

[76] F.H. Spedding, C.F. Miller, Journal of the American Chemical Society 74 (1952) 4195-4198.

[77] G.C. Fitzgibbon, D. Pavone, C.E. Holley, Jr., Journal of Chemical & Engineering Data 13 (1968) 547-548.

[78] L.R. Morss, C.M. Haar, S. Mroczkowski, The Journal of Chemical Thermodynamics 21 (1989) 1079-1083.

[79] A.A. Popova, A.S. Monaenkova, Zh. Fiz. Khim. 63 (1989) 2340.

[80] C. Hennig, Oppermann, H., Zeitschrift für Naturforschung B 53 (1998) 175–183.

[81] E.J.J. Huber, C.O. Matthews, C.E. Holley, Jr., Journal of the American Chemical Society 77 (1955) 6493-6494.

[82] F.H. Spedding, R.E. Eberts, A.W. Naumann, Technical Report ISC-934, US Atomic Energy Community, 1959.

[83] G.G. Gvelesiani, T.S. Yashvili, Zhurnal Neorganicheskoi Khimii 12 (1967) 3233.

[84] C. Hennig, Oppermann, H., Zeitschrift für Naturforschung B 52 (1997) 1517–1525.

[85] E.J.J. Huber, G.C. Fitzgibbon, C.E. Holley, Jr., Journal of Physical Chemistry 68 (1964) 2720-2722.

[86] G.C. Fitzgibbon, E.J.J. Huber, C.E. Holley, Jr., Journal of Chemical Thermodynamics 4 (1972) 349-358.

[87] C. Hennig, H. Oppermann, A. Blonska, Zeitschrift für Naturforschung Section BA Journal of Chemical Sciences 53 (1998) 1169-1179.

[88] E.J.J. Huber, C.E. Holley, Jr., Journal of the American Chemical Society 77 (1955) 1444-1445.

[89] E.J.J. Huber, E.L. Head, C.E. Holley, Jr., Journal of Physical Chemistry 60 (1956) 1457-1458.

[90] E.J.J. Huber, G.C. Fitzgibbon, C.E. Holley, Jr., Journal of Chemical Thermodynamics 3 (1971) 643-648.

[91] E.J.J. Huber, E.L. Head, C.E. Holley, Jr., The Journal of Physical Chemistry 61 (1957) 1021-1022.

[92] E.J.J. Huber, E.L. Head, C.E. Holley, Jr., The Journal of Physical Chemistry 60 (1956) 1582.

[93] J.M. Stuve, Heat of Formation of Europium Sesquioxide and Europium Trichloride, U.S. Bureau of Mines, 1965.

[94] Y.D. Tretyakov, A.R. Kaul, V.K. Portnoy, High Temperature Science 9 (1977) 61.

[95] N. Kimizuka, A. Yamamoto, H. Ohashi, T. Sugihara, T. Sekine, Journal of Solid State Chemistry 49 (1983) 65-76.

[96] A.R. Kaul, V.I. Kovalenko, Y.D. Tretyakov, Vestn. Mosk. Univ. Chemical Series hand. Dep. VINITI (1976) 235-276.

[97] S. Yamauchi, K. Fueki, N.C. Mukaibo, Bulletin of the Chemical Society of Japan 48 1039.

[98] A. Navrotsky, S.V. Ushakov, Thermodynamics of Oxide Systems Relevant to Alternative Gate Dielectrics. in: A.A. Demkov, A. Navrotsky, (Eds.), Materials Fundamentals of Gate Dielectrics, Springer, 2005, pp. 57-108.

[99] C. Laberty, Navrotsky, A., Rao, C. N. R., & Alphonse, P.", Journal of Solid State Chemistry 145 (1999) 77-87.

[100] J. Goudiakas, R.G. Haire, J. Fuger, The Journal of Chemical Thermodynamics 22 (1990) 577-587.

[101] S.V. Ushakov, K.B. Helean, A. Navrotsky, L.A. Boatner, Journal of Materials Research 16 (2001) 2623-2633.

[102] I.V. Tananaev, V.P. Orlovsky, J.M. Kurbanov, B.S. Halikov, S.O. Osman, V.I. Bulgakov, Reports of the Academy of Sciences of the Tajik SSR = Dokladhoi Akademiyai fanhoi RCC Tochikiston (USSR), 1974, pp. 42.

[103] K. Popa, R.J.M. Konings, Thermochimica acta 445 (2006) 49-52.

[104] K.S. Gavrichev, M.A. Ryumin, A.V. Tyurin, V.M. Gurevich, A.V. Khoroshilov, L.N. Komissarova, Thermochimica acta 535 (2012) 1-7.

[105] E. Lamb, and R. G. Donnelly, ORNL isotopic power fuels quarterly report for period ending June 30, 1973. No. ORNL--4174, Oak Ridge National Lab., Tenn.(USA), Oak Ridge National Lab., Tenn.(USA), 1973.

[106] M. Bolech, Cordfunke, E. H. P., Van Genderen, A. C. G., Van Der Laan, R. R., Janssen, F. J. J. G., & Van Miltenburg, J. C.. , Journal of Physics and Chemistry of Solids 58 (1997).

[107] A.V. Radha, S.V. Ushakov, A. Navrotsky, Journal of materials research 24 (2009) 3350-3357.

[108] S. Lutique, P. Javorskỳ, R.J.M. Konings, J.C. Krupa, A.C.G. van Genderen, J.C. van Miltenburg, F. Wastin, The Journal of Chemical Thermodynamics 36 (2004) 609-618.

[109] K.B. Helean, S.V. Ushakov, C.E. Brown, A. Navrotsky, J. Lian, R.C. Ewing, J.M. Farmer, L.A. Boatner, Journal of Solid State Chemistry 177 (2004) 1858-1866.

[110] S. Hayun, A. Navrotsky, Journal of Solid State Chemistry 187 (2012) 70-74.

[111] J. Lian, H.B. Helean, B.J. Kennedy, L.M. Wang, A. Navrotsky, R.C. Ewing, Journal of Physical Chemistry B 110 (2006) 2343-2350.

[112] A. Navrotsky, Thermochemistry of Perovskite-related oxides with high oxidation states: Superconductors, sensors, fuel cell materials, Pure Appl Chem, 1994, pp. 1759.

[113] J. Cheng, A. Navrotsky, X.-D. Zhou, H.U. Anderson, Journal of Materials Research 20 (2005) 191-200.

[114] J.J. Liang, Navrotsky, A., Ludwig, T., Seifert, H. J., & Aldinger, F, Journal of materials research 14 (1999) 130-137.

[115] E.H.P. Cordfunke, A.S. Booij, R.R. van der Laan, The Journal of Chemical Thermodynamics 30 (1998) 199-205.

[116] M. Bolech, Janssen, F. J. J. G., Booij, A. S., & Cordfunke, E. H. P., The Journal of Chemical Thermodynamics 28 (1996) 1319-1324.

[117] M. Bolech, Cordfunke, E. H. P., Van Genderen, A. C. G., Van der Laan, R. R., Janssen, F. J. J. G., & Van Miltenburg, J. C., Thermochimica acta 28 (1996) 235-261.

[118] V.E. Lamberti, M.A. Rodriguez, J.D. Trybulski, A. Navrotsky, ChemInform 28 (1997).

[119] N.I. Matskevich, R.W. McCallum, Thermochimica acta 342 (1999) 41-46.

[120] Z. Zhou, A. Navrotsky, Journal of materials research 7 (1992) 2920-2935.

[121] A.O.F. Sjåstad, H. Helean, K. B., Navrotsky, A., Thermochimica acta 550 (2012) 76-82.

[122] A. Olafsen, H. Fjellvag, S. Stolen, T. Atake, H. Kawaji, K. Matsuo, Journal of Chemical Thermodynamics 31 (1999) 433.

[123] D.A. Sverjensky, Geochimica et Cosmochimica Acta 48 (1984) 1127-1134.

[124] I.I. Diakonov, K. V. Ragnarsdottir, and B. R. Tagirov, Chemical geology 151 (1998) 327-347.

[125] R.D. Chirico, and Edgar F. Westrum The Journal of Chemical Thermodynamics 13 (1981) 519-525.

[126] L. Merli, B. Lambert, J. Fuger, Journal of Nuclear Materials 247 (1997) 172-176.

[127] E.H.P. Cordfunke, R.J.M. Konings, W. Ouweltjes, The Journal of Chemical Thermodynamics 22 (1990) 449-452.

[128] I.I. Diakonov, K.V. Ragnarsdottir, B.R. Tagirov, Chemical Geology 151 (1998) 327-347.

[129] L.R. Morss, C.W. Williams, Radiochimica Acta 66 (1994) 89.

[130] R.D. Chirico, Juliana Boerio-Goates, and Edgar F. Westrum Jr. , The Journal of Chemical Thermodynamics 13 (1981) 1087-1094.

[131] R.D. Chirico, and Edgar F. Westrum, The Journal of Chemical Thermodynamics 12 (1980) 311-327.

[132] R.D. Chirico, E.F. Westrum Jr, The Journal of Chemical Thermodynamics 12 (1980) 71-85.

[133] F.D. Rossini, D.W. Donald, Selected Values of Chemical Thermodynamic Properties, US Government Printng Office, Washington DC, 1952.

[134] J. Cheng, A. Navrotsky, Journal of Solid State Chemistry 178 (2005) 234-244.

[135] J. Cheng, A. Navrotsky, X.-D. Zhou, H.U. Anderson, Chemistry of Materials 17 (2005) 2197-2207.

[136] N. Kemik, Y. Takamura, A. Navrotsky, Journal of Solid State Chemistry 184 (2011) 2118-2123.

[137] J. Cheng, A. Navrotsky, Journal of Solid State Chemistry 177 (2004) 126-133.

[138] N. Navi, G. Kimmel, J. Zabicky, S.V. Ushakov, R. Shneck, M. Mintz, A. Navrotsky, Journal of the American Ceramic Society 94 (2011) 3112-3116.

[139] J. Bularzik, A. Navrotsky, Materials Research Society Symposium Proceedings 169 (1990) 61-64.

[140] J. Bularzik, A. Navrotsky, J. DiCarlo, J. Bringley, B. Scott, S. Trail, Journal of Solid State Chemistry 93 (1991) 418-429.

[141] J. DiCarlo, J. Bularzik, A. Navrotsky, Journal of Solid State Chemistry 96 (1992) 381-389.

[142] J. DiCarlo, A. Mehta, D. Banschick, A. Navrotsky, Journal of Solid State Chemistry 103 (1993) 186-192.

[143] T.R.S. Prasanna, A. Navrotsky, Journal of Solid State Chemistry 112 (1994) 192-195.

[144] S. Buyukkilic, T. Shvareva, A. Navrotsky, Solid State ionics 227 (2012) 17-22.

[145] S. Buyukkilic, S. Kim, A. Navrotsky, Angewandte Chemie International Edition 126 (2014) 9671-9675.

[146] W. Chen, T.A. Lee, A. Navrotsky, Journal of Materials Research 20 (2005) 144-150.

[147] W. Chen, A. Navrotsky, Journal of Materials Research 21 (2006) 3242-3251.

[148] W. Chen, A. Navrotsky, Y.P. Xiong, H. Yokokawa, Journal of the American Ceramic Society 90 (2007) 584-589.

[149] T.A. Lee, A. Navrotsky, I. Molodetsky, Journal of Materials Research 18 (2003) 908-918.

[150] T.A. Lee, A. Navrotsky, Journal of Materials Research 19 (2004) 1855-1861.

[151] T.A. Lee, C.R. Stanek, K.J. McClellan, J.N. Mitchell, A. Navrotsky, Journal of Materials Research 23 (2008) 1105-1112.

[152] T.B. Tran, A. Navrotsky, Chemistry of Materials 24 (2012) 4185-4191.

[153] T.B. Tran, A. Navrotsky, Physical Chemistry Chemical Physics 16 (2014) 2331-2337.

[154] M. Aizenshtein, T.Y. Shvareva, A. Navrotsky, Journal of the American Ceramic Society 93 (2010) 4124-4147.

[155] T.Y. Shvareva, V. Alexandrov, M. Asta, A. Navrotsky, Journal of Nuclear Materials 419 (2011) 72-75.

[156] S.V. Ushakov, A. Navrotsky, J.A. Tangeman, Materials Research Society Symposium Proceedings 1122 (2009) 11-16.

[157] M.P. Saradhi, S.V. Ushakov, A. Navrotsky, Royal Society of Chemistry Advances 2 (2012) 3328-3334.

[158] S. Hayun, T. Tran, J. Lian, A. Navrotsky, Acta Materialia 60 (2012) 4303-4310.

[159] Q.-J. Hong, S.V. Ushakov, A. Navrotsky, A.v.d. Walle, Acta Materialia In Press (2014).

[160] M.C. Wilding, A. Navrotsky, Journal of Non-Crystalline Solids 265 (2000) 238-251.

[161] Y. Linard, M.C. Wilding, A. Navrotsky, Geochimica et Cosmochimica Acta 72 (2008) 590-601.

[162] Y. Zhang, A. Navrotsky, H. li, L. Li, L.L. Davis, D.M. Strachan, Journal of Non-Crystalline Solids 296 (2001) 93-101.

[163] Y. Zhang, A. Navrotsky, J.A. Tangeman, J.K.R. Weber, Journal of Physics: Condensed Matter 15 (2003) S2343-S2355.

[164] Y. Zhang, A. Navrotsky, Journal of Materials Research 18 (2003) 1607-1613.

[165] Y. Zhang, A. Navrotsky, Journal of the American Ceramic Society 86 (2003) 1727-1732.

[166] S.V. Ushakov, C.E. Brown, A. Navrotsky, Journal of Materials Research 19 (2004) 693-696.

[167] S.V. Ushakov, A. Navrotsky, Y. Yang, S. Stemmer, K. Kukli, M. Ritala, M.A. Leskela, P. Fejes, A. Demkov, C. Wang, B.-Y. Nguyen, D. Triyoso, P. Tobin, Physica Status Solidi B 241 (2004) 2268-2278.

[168] R.M. Morcos, J. Tangeman, S.V. Ushakov, A. Navrotsky, Journal of the American Ceramic Society 91 (2008) 1088-1094.

[169] T.-J. Park, S. Li, A. Navrotsky, Journal of Materials Research 24 (2009) 3380-3386.

[170] T.-J. Park, A. Navrotsky, Journal of the American Ceramic Society 93 (2010) 2055-2061.

[171] P. Zhang, A. Navrotsky, Journal of Physical Chemistry C 112 (2008) 932-938.

[172] S. Chen, H.J. Avila-Paredes, S. Kim, J. Zhao, Z. Munir, A. Navrotsky, Physical Chemistry Chemical Physics 11 (2009) 3039-3042.

[173] S. Chen, G.C.C. Costa, S. Wang, Z.A. Munir, S. Kim, A. Navrotsky, Journal of the American Ceramic Society 94 (2011) 2181-2184.

[174] S. Hayun, T. Shvareva, A. Navrotsky, Journal of the American Ceramic Society 94 (2011) 3992-3999.

[175] S. Hayun, S.V. Ushakov, A. Navrotsky, Journal of the American Ceramic Society 94 (2011) 3679-3682.

[176] W. Zhou, S.V. Ushakov, A. Navrotsky, Journal of Materials Research 27 (2012) 1022-1028.

[177] L. Vradman, A. Navrotsky, Journal of the American Ceramic Society 96 (2013) 3202-3209.

[178] A.N.a.S.V. Ushakov, Thermodynamics of Oxide Systems Relevant to Alternative Gate Dielectrics. in: A.N. Alexander A. Demkov, (Ed.), Materials Fundamentals of Gate Dielectrics, Springer Science & Business Media, 2005, pp. 73.

[179] R. Shannon, Acta Crystallographica Section A 32 (1976) 751-767.

[180] P.J. Wilde, C.R.A. Catlow, Solid State Ionics 112 (1998) 173-183.

[181] S.V. Ushakov, Helean, K. B., Navrotsky, A., & Boatner, L. A, Journal of Materials Research 16 (2001).

[182] A. Navrotsky, Systematic Trends and Prediction of Enthalpies of Formation of Refractory Lanthanide and Actinide Ternary Oxide Phases. in: D.R. Spearing, G.L. Smith, R.L. Putnam, (Eds.),

Environmental Issues and Waste Management Technologies in the Ceramic and Nuclear Industries VI, American Ceramic Society, Westerville, Ohio, USA, 2000, pp. 137-146.

Graphical Abstract

Enthalpy of formation depends on ionic radius of rare earth and acidity of other components